

TYPE IA SUPERNOVA EXPLOSION MODELS

Wolfgang Hillebrandt¹ and Jens C. Niemeyer²

¹*Max-Planck-Institut für Astrophysik, Karl-Schwarzschild-Str. 1, 85740 Garching, Germany; e-mail: wfh@MPA-Garching.mpg.de*

²*University of Chicago, Enrico-Fermi Institute, 5640 South Ellis Ave., Chicago, Illinois 60637; e-mail: j-niemeyer@uchicago.edu*

Key Words stellar evolution, hydrodynamics

■ **Abstract** Because calibrated light curves of type Ia supernovae have become a major tool to determine the local expansion rate of the universe and also its geometrical structure, considerable attention has been given to models of these events over the past couple of years. There are good reasons to believe that perhaps most type Ia supernovae are the explosions of white dwarfs that have approached the Chandrasekhar mass, $M_{\text{chan}} \approx 1.39 M_{\odot}$, and are disrupted by thermonuclear fusion of carbon and oxygen. However, the mechanism whereby such accreting carbon-oxygen white dwarfs explode continues to be uncertain. Recent progress in modeling type Ia supernovae as well as several of the still open questions are addressed in this review. Although the main emphasis is on studies of the explosion mechanism itself and on the related physical processes, including the physics of turbulent nuclear combustion in degenerate stars, we also discuss observational constraints.

1. INTRODUCTION

Changes in the appearance of the night sky, visible with the naked eye, have always called for explanations (and speculations). But, although “new stars,” i.e. novae and supernovae, have been observed by humans for thousands of years, the modern era of supernova research began only about a century ago, on August 31, 1885, when Hartwig discovered a “nova” near the center of the Andromeda galaxy, which became invisible about 18 months later. In 1919, Lundmark estimated the distance of M31 to be about 7×10^5 ly, and by that time it became obvious that Hartwig’s nova had been several 1000 times brighter than a normal nova (Lundmark 1920). It was also Lundmark (1921) who first suggested an association between the supernova observed by Chinese astronomers in 1054 and the Crab nebula.

A similar event as S Andromeda was observed in 1895 in NGC 5253 (“nova” Z Centauri), and this time the “new star” appeared to be five times brighter than the entire galaxy. But it was not before 1934 that a clear distinction between classical

novae and supernovae was made (Baade & Zwicky 1934). Systematic searches, performed predominantly by Zwicky, lead to the discovery of 54 supernovae in the years up to 1956 and, owing to improved observational techniques, 82 further supernovae were discovered in the years from 1958 to 1963, all of course in external galaxies (e.g. Zwicky 1965).

Until 1937, spectrograms of supernovae were rare, and what was known seemed to be not too different from common novae. This changed with the very bright ($m_V \simeq 8.4$) supernova SN1937c in IC 4182, which had spectral features different from any object that had been observed before (Popper 1937). All the other supernovae discovered in the following years showed little dispersion in their maximum luminosity, and their postmaximum spectra looked similar at any given time. Based on this finding, Wilson (1939) and Zwicky (1938a) suggested supernovae be used as distance indicators.

In 1940 it became clear, however, that there exist at least two distinctly different classes of supernovae. SN 1940c in NGC 4725 had a spectrum different from all other previously observed supernovae for which good data were available at that time, leading Minkowski (1940) to introduce the names type I for those with spectra like SN 1937c and type II for SN 1940c-like events, representing supernovae without and with Balmer lines of hydrogen near maximum light.

Whether or not the spectral differences also reflect a different explosion mechanism was not known. In contrast, the scenario originally suggested by Zwicky (1938b), that a supernova occurs as the transition from an ordinary star to a neutron star and gains its energy from the gravitational binding of the newly born compact object, was for many years the only explanation. Hoyle & Fowler (1960) were the first to discover that thermonuclear burning in an electron-degenerate stellar core might trigger an explosion and (possibly) the disruption of the star. Together with the idea that the light curves could be powered by the decay-energy of freshly produced radioactive ^{56}Ni (Truran et al 1967, Colgate & McKee 1969), this scenario is now the generally accepted one for a subclass of all type I supernovae called type Ia. It is amusing to note that all supernovae (besides the Crab nebula) on which Zwicky had based his core-collapse hypothesis were in fact of type Ia and most likely belonged to the other group, whereas the first core-collapse supernova, SN1940c, was observed only about a year after he published his paper.

To be more precise, supernovae that do not show hydrogen lines in their spectra but a strong silicon P Cygni feature near maximum light are named type Ia (Wheeler & Harkness 1990). They are believed to be the result of thermonuclear disruptions of white dwarfs, either consisting of carbon and oxygen with a mass close to the Chandrasekhar mass, or of a low-mass C + O core mantled by a layer of helium, the so-called sub-Chandrasekhar mass models [see the recent reviews by Woosley (1997b), Woosley & Weaver (1994a, 1994b) and Nomoto et al (1994b, 1997)]. The main arguments in favor of this interpretation include: (a) the apparent lack of neutron stars in some of the historical galactic supernovae (e.g. SN1006, SN 1572, SN1604); (b) the homogeneous appearance of this subclass; (c) the excellent fits to the light curves, which can be obtained from the simple assumption that a few tenths of a solar mass of ^{56}Ni is produced during the explosion; and

(*d*) the good agreement with the observed spectra of typical type Ia supernovae. Several of these observational aspects are discussed in some detail in Section 2, together with their cosmological implications. Models of light curves and spectra are reviewed in Section 3, and questions concerning the nature of the progenitor stars are addressed in Section 4.

But having good arguments in favor of a particular explosion scenario does not mean that this scenario is indeed the right one. Besides that, one would like to understand the physics of the explosion, the fact that the increasing amount of data also indicates that there is a certain diversity among the type Ia supernovae seems to contradict a single class of progenitor stars or a single explosion mechanism. Moreover, the desire for using them as distance indicators makes it necessary to search for possible systematic deviations from uniformity. Here, again, theory can make important contributions. In Section 5, therefore, we discuss the physics of thermonuclear combustion, its implementation into numerical models of exploding white dwarfs, and the results of recent computer simulations. A summary and conclusions follow in Section 6.

2. OBSERVATIONS

The efforts to systematically obtain observational data of SNe Ia near and far have gained tremendous momentum in recent years. This is primarily a result of the unequaled potential of SNe Ia to act as “standardizable” candles (Branch & Tammann 1992, Riess et al 1996, Hamuy et al 1995, Tripp 1998) for the measurement of the cosmological expansion rate (Hamuy et al 1996b, Branch 1998) and its variation with look-back time (Perlmutter et al 1999, Schmidt et al 1998, Riess et al 1998). For theorists, this development presents both a challenge to help understand the correlations among the observables and an opportunity to use the wealth of new data to constrain the zoo of existing explosion models. There exist a number of excellent reviews about SNe Ia observations in general (Filippenko 1997b), their spectral properties (Filippenko 1997a), photometry in the infrared (IR) and optical bands (Meikle et al 1996, 1997), and their use for measuring the Hubble constant (Branch 1998). Recent books that cover a variety of observational and theoretical aspects of type Ia supernovae are Ruiz-Lapuente et al (1997) and Niemeyer & Truran (2000). Below, we highlight those aspects of SN Ia observations that most directly influence theoretical model building at the current time.

2.1 General Properties

The classification of SNe Ia is based on spectroscopic features: the absence of hydrogen absorption lines, distinguishing them from type II supernovae, and the presence of strong silicon lines in the early and maximum spectrum, classifying them as type Ia (Wheeler & Harkness 1990).

The spectral properties, absolute magnitudes, and light curve shapes of the majority of SN Ia are remarkably homogeneous, exhibiting only subtle spectroscopic and photometric differences (Branch & Tammann 1992, Hamuy et al 1996c,

Branch 1998). It was believed until recently that approximately 85% of all observed events belonged to this class of normal [“Branch-normal” (Branch et al 1993)] SNe Ia, represented for example by SNe 1972E, 1981B, 1989B, and 1994D. However, the peculiarity rate can be as high as 30% as suggested by Li et al (2000).

The optical spectra of normal SN Ia contain neutral and singly ionized lines of Si, Ca, Mg, S, and O at maximum light, indicating that the outer layers of the ejecta are mainly composed of intermediate mass elements (Filippenko 1997b). Permitted Fe II lines dominate the spectra roughly 2 weeks after maximum when the photosphere begins to penetrate Fe-rich ejecta (Harkness 1991). In the nebular phase of the light curve tail, beginning approximately 1 month after peak brightness, forbidden Fe II, Fe III, and Co III emission lines become the dominant spectral features (Axelrod 1980). Some Ca II remains observable in absorption even at late times (Filippenko 1997a). The decrease of Co lines (Axelrod 1980) and the relative intensity of Co III and Fe III (Kuchner et al 1994) give evidence that the light curve tail is powered by radioactive decay of ^{56}Co (Truran et al 1967, Colgate & McKee 1969).

The early spectra can be explained by resonant scattering of a thermal continuum with P Cygni-profiles whose absorption component is blueshifted according to ejecta velocities of up to a few times 10^4 km s^{-1} , rapidly decreasing with time in the early phase (Filippenko 1997a). Different lines have different expansion velocities (Patat et al 1996), which suggests a layered structure of the explosion products.

Photometrically, SN Ia rise to maximum light in a period of approximately 20 days (Riess et al 1999b) reaching

$$M_B \approx M_V \approx -19.30 \pm 0.03 + 5 \log(H_0/60) \quad (1)$$

with a dispersion of $\sigma_M \leq 0.3$ (Hamuy et al 1996b). It is followed by a first rapid decline of about three magnitudes in a matter of 1 month. Later, the light curve tail falls off in an exponential manner at a rate of approximately one magnitude per month. In the I-band, normal SNe Ia rise to a second maximum approximately 2 days after the first maximum (Meikle et al 1997).

It is especially interesting that the two most abundant elements in the universe, hydrogen and helium, have not been unambiguously detected in SN Ia spectra (Filippenko 1997a; for a possible identification of He, see Meikle et al 1996), and there are no indications for radio emission of SNe Ia. Cumming et al (1996) failed to find any signatures of H in the early time spectrum of SN 1994D and used this fact to constrain the mass accretion rate of the progenitor wind (Lundqvist & Cumming 1997). The later spectrum of SN 1994D also did not exhibit narrow H α features (Filippenko 1997b). Another direct constraint for the progenitor system accretion rate comes from the nondetection of radio emission from SN 1986G (Eck et al 1995), used by Boffi & Branch (1995) to rule out symbiotic systems as a possible progenitor of this event.

2.2 Diversity and Correlations

Early suggestions (Pskovskii 1977, Branch 1981) that the existing inhomogeneities among SN Ia observables are strongly intercorrelated are now established beyond

doubt (Hamuy et al 1996a, Filippenko 1997a). Branch (1998) offers a recent summary of correlations between spectroscopic line strengths, ejecta velocities, colors, peak absolute magnitudes, and light curve shapes. Roughly speaking, SNe Ia appear to be arrangeable in a one-parameter sequence according to explosion strength, wherein the weaker explosions are less luminous, are redder, and have a faster declining light curve and slower ejecta velocities than the more energetic events (Branch 1998). The relation between the width of the light curve around maximum and the peak brightness is the most prominent of all correlations (Pskovskii 1977, Phillips 1993). Parameterized either by the decline rate Δm_{15} (Phillips 1993, Hamuy et al 1996a), a “stretch parameter” (Perlmutter et al 1997), or a multi-parameter nonlinear fit in multiple colors (Riess et al 1996), it was used to renormalize the peak magnitudes of a variety of observed events, substantially reducing the dispersion of absolute brightnesses (Riess et al 1996, Tripp 1998). This correction procedure is a central ingredient of all current cosmological surveys that use SNe Ia as distance indicators (Perlmutter et al 1999, Schmidt et al 1998).

SN 1991bg and SN 1992K are well-studied examples for red, fast, and subluminal supernovae (Filippenko et al 1992a, Leibundgut et al 1993, Hamuy et al 1994, Turatto et al 1996). Their V-, I-, and R-band light curve declined unusually quickly, skipping the second maximum in I, and their spectrum showed a high abundance of intermediate mass elements (including Ti II) with low expansion velocities but only little iron (Filippenko et al 1992a). Models for the nebular spectra and light curve of SN 1991bg consistently imply that the total mass of ^{56}Ni in the ejecta was very low ($\sim 0.07 M_{\odot}$) (Mazzali et al 1997a). On the other side of the luminosity function, SN 1991T is typically mentioned as the most striking representative of bright, energetic events with broad light curves (Phillips et al 1992, Jeffery et al 1992, Filippenko et al 1992b, Ruiz-Lapuente et al 1992, Spyromilio et al 1992). Rather than the expected Si II and Ca II, its early spectrum displayed high-excitation lines of Fe III but returned to normal a few months after maximum (Filippenko et al 1992b).

Peculiar events like SN 1991T and SN 1991bg were suggested as belonging to subgroups of SNe Ia different from those of the normal majority, created by different explosion mechanisms (Mazzali et al 1997a, Filippenko et al 1992b, Fisher et al 1999). Until recently, the overall SN Ia luminosity function seemed to be very steep on the bright end (Vaughan et al 1995), implying that “normal” events are essentially the brightest whereas the full class may contain a large number of undetected subluminal SNe Ia (Livio 1999). New results (Li et al 2000) indicate, however, that the luminosity function may be shallower than anticipated.

There is also mounting evidence that SN Ia observables are correlated with the host stellar population (Branch 1998). SNe Ia in red or early type galaxies show, on average, slower ejecta velocities and faster light curves, and they are dimmer by ≈ 0.2 – 0.3 mag than those in blue or late-type galaxies (Hamuy et al 1995, 1996a; Branch et al 1996). The SN Ia rate per unit luminosity is nearly a factor of 2 higher in late-type galaxies than in early type ones (Cappellaro et al

1997). In addition, the outer regions of spirals appear to give rise to similarly dim SNe Ia as ellipticals whereas the inner regions harbor a wider variety of explosion strengths (Wang et al 1997). When corrected for the difference in light curve shape, the variation of absolute magnitudes with galaxy type vanishes along with the dispersion of the former. This fact is crucial for cosmological SN Ia surveys, making the variations with stellar population consistent with the assumption of a single explosion strength parameter (Perlmutter et al 1999, Riess et al 1998).

2.3 Nearby and Distant SNe Ia

Following a long and successful tradition of using relatively nearby [$z \leq 0.1$, comprised mostly of the sample discovered by the Calán/Tololo survey (Hamuy et al 1996a)] SNe Ia for determining the Hubble constant (Branch 1998), the field of SN Ia cosmology has recently seen a lot of activity, expanding the range of observed events out to larger redshift, $z \approx 1$. Systematic searches involving a series of wide-field images taken at epochs separated by 3–4 weeks, in addition to prescheduled follow-up observations to obtain detailed spectroscopy and photometry of selected events, have allowed two independent groups of observers—the Supernova Cosmology Project (SCP) (Perlmutter et al 1999) and the High- z Supernova Search Team (Schmidt et al 1998)—to collect data of more than 50 high-redshift SNe. Extending the Hubble diagram out to $z \approx 1$, one can, given a sufficient number of data points over a wide range of z , determine the density parameters for matter and cosmological constant, Ω_M and Ω_Λ , independently (Goobar & Perlmutter 1995), or, in other words, constrain the equation of state of the universe (Garnavich et al 1998). Both groups come to a spectacular conclusion (Riess et al 1998, Perlmutter et al 1999): The distant SNe are too dim by ≈ 0.25 mag to be consistent with a purely matter-dominated, flat or open Friedmann-Robertson-Walker universe. Interpreted as being a consequence of a larger-than-expected distance, this discrepancy can be resolved only if Ω_Λ is non-zero, implying the existence of an energy component with negative pressure. In fact, the SN Ia data is consistent with a spatially flat universe made up of two parts vacuum energy and one part matter.

Both groups discuss in detail the precautions that were taken to avoid systematic contaminations of the detection of cosmological acceleration, including SN Ia evolution, extinction, and demagnification by gravitational lensing. All of these effects would, in all but the most contrived scenarios, give rise to an increasing deviation from the $\Omega_\Lambda = 0$ case for higher redshift, whereas the effect of a non-zero cosmological constant should become less significant as z grows. Thus, the degeneracy between a systematic overestimation of the intrinsic SN Ia luminosity and cosmological acceleration can be broken when sufficiently many events at $z \geq 0.85$ are observed (Filippenko & Riess 1999). Meanwhile, the only way to support the cosmological interpretation is by “...adding to the list of ways in which they are similar while failing to discern any way in which they are different”

(Riess et al 1999a). This program has been successful until recently: The list of similarities between nearby and distant SNe Ia includes spectra near maximum brightness (Riess et al 1998) and the distributions of brightness differences, light curve correction factors, and $B - V$ color excesses of both samples (Perlmutter et al 1999). Moreover, although the nearby sample covers a range of stellar populations similar to the one expected out to $z \approx 1$, a separation of the low- z data into subsamples arising from different progenitor populations shows no systematic shift of the distance estimates (Filippenko & Riess 2000). However, a recent comparison of the rise times of more than 20 nearby SNe (Riess et al 1999b) with those determined for the SCP high-redshift events gives preliminary evidence for a difference of roughly 2.5 days. This result was disputed by Aldering et al (2000) who conclude that the rise times of local and distant supernovae are statistically consistent.

2.4 Summary: Observational Requirements for Explosion Models

To summarize the main observational constraints, any viable scenario for the SN Ia explosion mechanism has to satisfy the following (necessary but probably not sufficient) requirements:

1. *Agreement of the ejecta composition and velocity with observed spectra and light curves.* In general, the explosion must be sufficiently powerful (i.e. produce enough ^{56}Ni) and produce a substantial amount of high-velocity intermediate mass elements in the outer layers. Furthermore, the isotopic abundances of “normal” SNe Ia must not deviate significantly from those found in the solar system.
2. *Robustness of the explosion mechanism.* In order to account for the homogeneity of normal SNe Ia, the standard model should not give rise to widely different outcomes, depending on the fine-tuning of model parameters or initial conditions.
3. *Intrinsic variability.* Although the basic model should be robust with respect to small fluctuations, it must contain at least one parameter that can plausibly account for the observed sequence of explosion strengths.
4. *Correlation with progenitor system.* The explosion strength parameter must be causally connected with the state of the progenitor white dwarf in order to explain the observed variations as a function of the host stellar population.

3. LIGHT CURVE AND SPECTRA MODELING

Next we discuss the problem of coupling the interior physics of an exploding white dwarf to what is finally observed, namely light curves and spectra, by means of

radiative transfer calculations. For many astrophysical applications, this problem is not solved, and SN Ia are no exceptions. In fact, radiation transport is even more complex in type Ia than for most other cases.

A rough sketch of the processes involved can illustrate some of the difficulties (see, e.g. Mazzali & Lucy 1993, Eastman & Pinto 1993). Unlike most other objects we know in astrophysics, SN Ia do not contain any hydrogen. Therefore the opacities are always dominated either by electron scattering (in the optical) or by a huge number of atomic lines [in the ultraviolet (UV)]. In the beginning, the supernova is an opaque expanding sphere of matter into which energy is injected from radioactive decay. This could happen in an inhomogeneous manner, as is discussed later. As the matter expands, diffusion times eventually get shorter than the expansion time and the supernova becomes visual. However, because the star is rapidly expanding, the Doppler shift of atomic lines causes important effects. For example, a photon emitted somewhere in the supernova may find the surrounding matter more or less transparent until it finds a line Doppler shifted such that it is trapped in that line and scatters many times. As a consequence, the spectrum might look thermal although the photon “temperature” has nothing in common with the matter temperature.

It is also obvious that radiation transport in SN Ia is nonlocal and that the methods used commonly in models of stellar atmospheres need refinements. As a consequence, there is no agreement yet among the groups modeling light curves and spectra as to what the best approach is. Therefore it can happen that even if the same model for the interior physics of the supernova is inserted into one of the existing codes for modeling light curves and spectra, the predictions for what should be “observed” could be different—again an unpleasant situation. Things get even worse because all such models treat the exploding star as being spherically symmetric, an assumption that is at least questionable, given the complex combustion physics discussed below.

In the following subsections we outline some of the commonly used numerical techniques and also discuss their predictions for SN Ia spectra and light curves. For more details on the techniques used by the various groups, we refer readers to the articles by Eastman (1997), Blinnikov (1997), Pinto (1997), Baron et al (1997), Mazzali et al (1997b), Höflich et al (1997), and Ruiz-Lapuente (1997).

3.1 Radiative Transfer in Type Ia Supernovae

In principle, the equations that have to be solved are well known, either in the form of the Boltzmann transport equation for photons or as a transport equation for the monochromatic intensities. However, to solve this time-dependent, frequency-dependent radiation transport problem, including the need to treat the atoms in non-local thermodynamic equilibrium (NLTE), is expensive, even in spherically symmetric situations. Therefore, approximations of various kinds are usually made which give rise to controversial discussions.

Conceptually, it is best to formulate and solve the transport equation in the co-moving (Lagrangian) frame (cf. Mihalas & Weibel Mihalas 1984). This makes the transport equation appear simpler, but it causes problems in calculating the “co-moving” opacity, in particular if the effect of spectral lines on the opacity of an expanding shell of matter is important, as in the case of SN Ia (Karp et al 1977).

There are different ways to construct approximate solutions of the transport equation. One can integrate over frequency and replace the opacity terms by appropriate means, leaving a single (averaged) transport equation. Unfortunately, in order to compute the flux-mean opacity, one has to know the solution of the transport equation. Frequently the flux mean is replaced, for example, by the Rosseland mean, allowing for solutions, but at the expense of consistency (see, e.g., Eastman 1997).

Another way out is to replace the transport equation by its moment expansion, introducing, however, the problem of closure. In its simplest form, the diffusion approximation, the radiation field is assumed to be isotropic, the time rate of change of the flux is ignored, and the flux is expressed in terms of the gradient of the mean intensity of the radiation field. Replacing the mean intensity by the Planck function and closing the moment expansion by relating the radiation energy density and pressure via an Eddington factor (equal to one third for isotropic radiation) finally leads to a set of equations that can be solved (Mihalas & Weibel Mihalas 1984).

Again, this simple approach has several obvious shortcomings. First, the transition from an optically thick to thin medium at the photosphere requires a special treatment mainly because the radiation field is no longer isotropic. One can compensate for this effect by putting in either a flux limiter or a variable Eddington factor to describe the transition from diffusion to free streaming, but both approaches are not fully satisfactory because it is difficult to calibrate the newly invented parameters (e.g. Kunasz 1984, Fu 1987, Blinnikov & Nadyoshin 1991, Mair et al 1992, Stone et al 1992, Yin & Miller 1995).

Alternatively, one can bin frequency space into groups and solve the set of fully time-dependent coupled monochromatic transport equations for each bin. In this approach, the problem remains of computing average opacities for each frequency bin. Moreover, because of computer limitations, in all practical applications the number of bins cannot be large, which introduces considerable errors, given the strong frequency dependence of the line-opacities (Blinnikov & Nadyoshin 1991, Eastman 1997) (see also Figure 1).

Finally, in order to get synthetic spectra one might apply Monte-Carlo techniques, as was done by Mazzali et al (1997b) and Lucy (1999). Here the assumption is that the supernova envelope is in homologous spherical expansion and that the luminosity and the photospheric radius are given. The formation of spectral lines is then computed by considering the propagation of a wave packet emitted from the photosphere subject to electron scattering and interaction with lines. Line formation is assumed to occur by coherent scattering, and the line profiles and escape probabilities are calculated in the Sobolev approximation. Although this approach

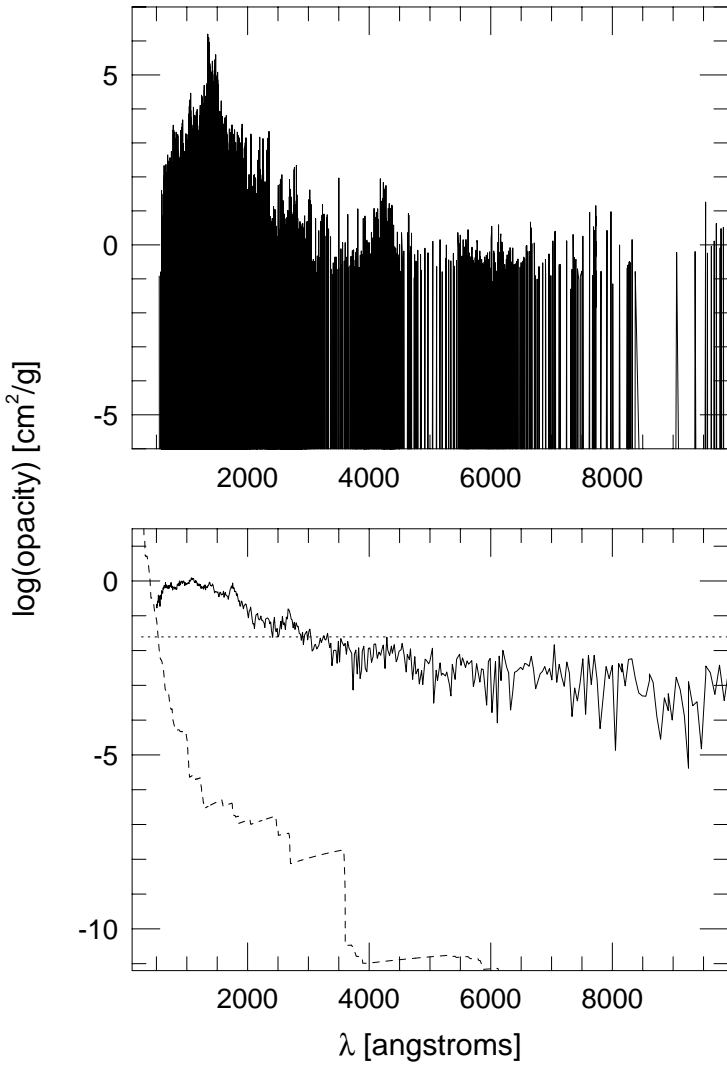


Figure 1 Mass opacity in a hot (23,000 K) plasma of cobalt at a density of 10^{-12} g/cm^3 . The upper plot shows the line opacities (calculated by Iglesias, Rogers & Wilson (1987) with OPAL), the lower one the bound-free (*long dashed*), electron scattering (*short dashed*), and the “line expansion opacity” (*solid curve*). (Courtesy of R. Eastman 1999, personal communication)

appears to be a powerful tool to get synthetic spectra, it lacks consistency because the properties of the photosphere have to be calculated by other means.

But having a numerical scheme at hand to solve the transport equation is not sufficient. It is even more important to have accurate opacities. The basic problem, namely that at short wavelengths the opacity is dominated by a huge number of weak lines, was mentioned before. In practice this means that because the list included in anyone's code is certainly incomplete and the available information may not always be accurate, it is difficult to estimate possible errors. Moreover, there is no general agreement among the different groups calculating SN Ia light curves and spectra on how to correct the opacities for Doppler shifts of the lines, caused by the expansion of the supernova. The so-called "expansion opacity" (see Figure 1) that should be used in approaches based on the diffusion equation as well as on moment expansions of the transport equation is still controversial (Pauldrach et al 1996, Blinnikov 1997, Baron et al 1997, Eastman 1997, Hoefflich et al 1997, Mazzali et al 1997b, Pinto 1997).

Other open questions include the relative importance of absorption and scattering of photons in lines, and whether one can calculate the occupation numbers of atomic levels in equilibrium or whether it has to be calculated by means of the Saha-equation (Pauldrach et al 1996, Nugent et al 1997, Hoefflich et al 1998b).

3.2 Results of Numerical Studies

Despite the problems discussed in the previous subsection, radiation hydrodynamic models have been used widely as a diagnostic tool for SN Ia. These studies include computations of γ -ray (Burrows & The 1990, Müller et al 1991, Burrows et al 1991, Shigeyama et al 1993, Ruiz-Lapuente et al 1993b, Timmes & Woosley 1997, Hoefflich et al 1998a, Watanabe et al 1999), UV and optical rays (Branch & Venkatakrishna 1986; Ruiz-Lapuente et al 1992; Nugent et al 1995, 1997; Pauldrach et al 1996; Hoefflich et al 1997; Hatano et al 1998; Hoefflich et al 1998b; Lentz et al 1999a,b; Fisher et al 1999; Lucy 1999) and of infrared light curves and spectra (Spyromilio et al 1994, Hoefflich 1995, Wheeler et al 1998). All studies are based on the assumption, that the explosion remains on average spherically symmetric, an assumption that is questionable, as is discussed in Section 5. Although spherical symmetry might be a good approximation for temperatures, densities, and velocities, the spatial distribution of the products of explosive nuclear burning is expected to be nonspherical, and it is the distribution of the heavier elements, both in real and in velocity space, that determines to a large extent light curves and spectra.

With the possible exception of SN 1991T, where a $2-3\sigma$ detection of the ^{56}Co decay lines at 847 keV and 1238 keV has been reported (Morris et al 1997; but see also Leising et al 1995), only upper limits on γ -ray line emission from SN Ia are known. On the basis of the models this is not surprising because the flux limits of detectors such as COMPTEL on GRO [10^{-5} photons per cm^2 and second (Schoenfelder et al 1996)] allows detections out to distances of about 15 Mpc in

the most favorable cases, i.e. delayed-detonation models producing lots of ^{56}Ni in the outer parts of the supernova (Timmes & Woosley 1997). In fact, the tentative detection of decay lines from SN 1991T at a distance of about 13 Mpc can be explained by certain delayed-detonation models and was even predicted by some of them (Müller et al (1991), see also Section 5).

Synthetic (optical and UV) spectra of hydrodynamic models of SN Ia have been computed by several groups (Hoeftlich & Khokhlov 1996, Nugent et al 1997) and have been compared with the observations. The bottom line of these investigations is that Chandrasekhar-mass deflagration models are in good agreement with observations of Branch-normals such as SN 1992A and SN 1994D (Hoeftlich & Khokhlov 1996, Nugent et al 1997), and delayed detonation are equally good. The reason is that in both classes of models, the burning front starts by propagating out slowly, giving the star some time to expand. The front then speeds up to higher velocities, i.e. to a fair fraction of the sound velocity for deflagration models and to supersonic velocity for detonations, which is necessary to match the observed high velocities of the ejecta. But as far as the amount of radioactive Ni is concerned, the predictions of both classes of models are not too different (Nugent et al 1997). It also appears that sub-Chandrasekhar models cannot explain the observed UV flux and the colors of normal SNe Ia (Khokhlov et al 1993). Moreover, although sub-Chandrasekhar models eject considerable amounts of He, according to the synthetic spectra, He lines should not be seen, eliminating them as a tool to distinguish between the models (Nugent et al 1997).

In the IR, SN Ia do show nonmonotonic behavior (Elias et al 1985), and as for the bolometric light curves, a correlation between peak brightness and light curve shape seems to exist (Contardo & Leibundgut 1998, Contardo 1999). Therefore calculations of IR light curves and spectra are of importance, and they might prove to be a good diagnostic tool. Broad-band IR light curves have been computed by Hoeftlich et al (1995) with the result that the second IR peak can be explained as an opacity effect. Although the fits were not perfect, the general behavior, again, was consistent with both the deflagration and the delayed-detonation models. Detailed early IR spectra have been calculated only recently (Wheeler et al 1998), and the models provide a good physical understanding of the spectra. Again, a comparison between several of the delayed-detonation models and SN 1994D gave good agreement, but one might suspect that certain deflagrations would do equally well. However, in principle, synthetic IR spectra are sensitive to the boundary between explosive C and O and between complete and incomplete Si burning (Wheeler et al 1998) and should provide some information on the progenitors and the explosion mechanism.

In conclusion, models of SN Ia light curves and spectra can fit the observations well, but so far, their predictive power is limited. The fact that multidimensional effects are ignored and that the opacities as well as the radiative-transfer codes have obvious shortcomings makes it difficult to derive strong constraints on the explosion mechanism. It appears, however, that although it seems to be difficult

to distinguish between pure deflagrations and delayed detonations on the basis of synthetic light curves and spectra, sub-Chandrasekhar models cannot fit normal SN Ia equally well.

4. PROGENITOR SYSTEMS

In contrast to supernovae from collapsing massive stars, for which in two cases the progenitor star was identified and some of its properties could be inferred directly from observations [SN1987A in the Large Magellanic Cloud (Blanco 1987, Gilmozzi 1987, Gilmozzi et al 1987, Hillebrandt et al 1987) and SN1993J in M81 (Benson et al 1993, Schmidt et al 1993, Nomoto et al 1993, Podsiadlowski 1993)], there is not a single case known where we have this kind of information for the progenitor of a SN Ia. This is not too surprising given the fact that their progenitors are most likely faint compact dwarf stars and not red or blue supergiants. Therefore we must rely on indirect means to determine their nature.

The standard procedure is to eliminate all potential candidates if some of their properties disagree with either observations or physical principles, and to hope that a single and unique solution is left. Unfortunately, for the progenitors of type Ia supernovae, this cannot be done unambiguously, the problem being the lack of strong candidates that pass all possible tests beyond doubt.

In this section, we first repeat the major constraints that must be imposed on the progenitor systems and then discuss in some detail the presently favored candidates, Chandrasekhar-mass C + O white dwarfs and low-mass C + O white dwarf cores embedded in a shell of helium. It is shown, however, that even if we could single out a particular progenitor system, this would narrow the parameter space for the initial conditions at the onset of the explosion but might not determine them sufficiently well, in particular if we are aiming at a quantitative understanding. Some of the discussion given below follows recent reviews of Renzini (1996) and Livio (1999).

4.1 Observational Constraints on Type Ia Progenitors

As discussed in Section 2, SNe Ia are (spectroscopically) defined by the absence of emission lines of hydrogen and the presence of a (blueshifted) Si II absorption line with a rest wavelength of 6355-Å near-maximum light. The first finding requires that the atmosphere of the exploding star contains no or at most $0.1 M_{\odot}$ of hydrogen, and the second one indicates that some nuclear processing takes place and that products of nuclear burning are ejected in the explosion. Mean velocities of the ejecta, as inferred from spectral fits, are around 5000 km s^{-1} and peak velocities exceeding $20,000 \text{ km s}^{-1}$ are observed, which is consistent with fusing about $1 M_{\odot}$ of carbon and oxygen into Fe group elements or intermediate-mass elements such as Si or Ca. The presence of some UV flux, the width of the peak of the early light

curve, and the fact that radioactive-decay models ($^{56}\text{Ni} \rightarrow ^{56}\text{Co} \rightarrow ^{56}\text{Fe}$) can fit the emission very well all point toward compact progenitor stars with radii of less than about 10,000 km.

After about 2 weeks, the typical SN Ia spectrum changes from being dominated by lines of intermediate-mass nuclei to being dominated by Fe II. Because a Co III feature is identified at later stages, this adds evidence to the interpretation that they are indeed thermonuclear explosions of compact stars, leaving the cores of stars with main sequence masses near $6\text{--}8 M_{\odot}$ or white dwarfs as potential candidates. Moreover, the energetics of the explosion and the spectra seem to exclude He white dwarfs (Nomoto & Sugimoto 1977, Woosley et al 1986), mainly because such white dwarfs would undergo very violent detonations.

Next one notes that most SNe Ia, of the order of 85%, have similar peak luminosities, light curves, and spectra. The dispersion in peak blue and visual brightness is only of the order of 0.2–0.3 mag, calling for a homogeneous class of progenitors. It is mainly this observational fact that seems to single out Chandrasekhar-mass white dwarfs as their progenitors. Because the ratio of energy to mass determines the velocity profile of the exploding star, the homogeneity would be explained in a natural way. However, as discussed in Section 2, there exist also significant differences among the various SNe Ia, which may indicate that this simple interpretation is not fully correct. The difference in peak brightness, ranging from subluminal events such as SN 1991bg in NGC 4374 ($B_{\text{max}} = -16.54$) (Turatto et al 1996), compared with the mean of the Branch-normals of $B_{\text{max}} \simeq -19$ (Hamuy et al 1996c) to bright ones such as SN 1991T, which was about 0.5 mag brighter in B than a typical type Ia in the Virgo cluster (Mazzali et al 1995), is commonly attributed to different ^{56}Ni masses produced in the explosion. They range from about $0.07 M_{\odot}$ for SN 1991bg (see, e.g., Mazzali et al 1997a) to at least $0.92 M_{\odot}$ for SN 1991T (Khokhlov et al 1993; but see also Fisher et al 1999), with typically $0.6 M_{\odot}$ for normal SNe Ia (Hoeftlich & Khokhlov 1996, Nugent et al 1997). It is hard to see how this large range can be accommodated in a single class of models.

The stellar populations in which SNe Ia show up include spiral arms as well as elliptical galaxies, with some weak indication that they might be more efficiently produced in young populations (Bartunov et al 1994). Again, if we insist on a single class of progenitors, the very fact that they do occur in ellipticals would rule out massive stars as potential candidates. On the other hand, the observations may tell us that there is not a unique class of progenitors. In particular, the fact that the bright and slowly declining ones (such as SN 1991T) are absent in an elliptical and S0 galaxies may point toward different progenitor classes (Hamuy et al 1996c).

All in all, the observational findings summarized so far are consistent with the assumption that type Ia supernovae are the result of thermonuclear disruptions of white dwarfs, C + O white dwarfs being the favored model. The diversity among them must then be attributed to the history and nature of the white dwarf prior to the explosion and/or to the physics of thermonuclear burning during the event. The

possibility cannot be excluded, however, that at least some SNe Ia have a different origin, such as accretion-induced collapse of massive O-Ne-Mg (or O-Ne) white dwarfs for SN 1991bg-like objects (Nomoto et al 1994a, 1995, 1996; Fryer et al 1999). Also it is not clear whether there is a clear-cut distinction between type Ib/c supernovae, defined by the absence of the Si II feature, and the (faint) SNe Ia. The former are believed to reflect the core collapse of a massive star, its hydrogen-rich envelope being peeled off because of mass loss in a binary system. For example, SN1987K started out as a SN II with H lines in its spectrum but changed into a SN Ib/c-like spectrum after 6 months (Filippenko 1988), supporting this interpretation. It should be noted that SN 1991bg-like objects are not often observed, but that this may well be a selection effect. Suntzeff (1996), for example, argues that up to 40% of all type Ia's could perhaps belong to that subgroup.

4.2 Presupernova Evolution of Binary Stars

In spite of all these uncertainties, it is the current understanding and belief that the progenitors of SNe Ia are C + O white dwarfs in binary systems evolving to the stage of explosion by mass overflow from the companion (single-degenerate scenario) or by the merger of two white dwarfs (double-degenerate scenario). Binary evolution of some sort is necessary because C + O white dwarfs are typically born with a mass around $0.6 M_{\odot}$ (Heuer et al 1998) but need either to be near the Chandrasekhar mass or to accumulate a shell of helium in order to explode. In this subsection, we summarize the arguments in favor and against both scenarios.

Double-degenerates as potential type Ia progenitors had many ups and downs in the past, beginning with the classic papers of Iben & Tutukov (1984) and Webbink (1984). The arguments in favor are that such binaries should exist as a consequence of stellar evolution, they would explain very naturally the absence of hydrogen, and they could, in principle, be an easy way to approach a critical mass. In fact, several candidate systems of binary white dwarfs have recently been identified, but most of the short-period ones (at present eight systems are known with orbital periods of less than half a day), which could merge in a Hubble time because of the emission of gravitational radiation, have a mass less than M_{chan} (Saffer et al 1998; for a recent review, see Livio 2000). There is only one system known [KPD 0422 + 5421 (Koen et al 1998)] with a mass which, within the errors, could exceed M_{chan} , a surprisingly small number. Nonetheless, it is argued that from population synthesis one could arrive at about the right frequency of sufficiently massive mergers (Livio 2000).

Besides the lack of convincing direct observational evidence for sufficiently many appropriate binary systems, the homogeneity of "typical" SNe Ia may be an argument against this class of progenitors. It is not easy to see how the merging of two white dwarfs of (likely) different mass, composition, and angular momentum with different impact parameters, etc, will always lead to the same burning conditions and, therefore, the production of a nearly equal amount of ^{56}Ni . Moreover,

some investigations of white dwarf mergers seem to indicate that an off-center ignition will convert carbon and oxygen into oxygen, neon, and magnesium, leading to gravitational collapse rather than a thermonuclear disruption (Nomoto & Iben 1985; Woosley & Weaver 1986a; Saio & Nomoto 1985, 1998; Mochkovitch & Livio 1990). Finally, based on their galactic chemical evolution model, Kobayashi et al (1998) claim that double-degenerate mergers lead to inconsistencies with the observed O/Fe as a function of metallicity, but this statement is certainly model dependent. In any case, mergers might, if they are not responsible for the bulk of the SNe Ia, still account for some peculiar ones, such as the superluminous SN 1991T-like explosions.

Single-degenerate models are in general favored today. They consist of a low-mass white dwarf accreting matter from the companion star until either it reaches M_{chan} or a layer of helium has formed on top of its C + O core that can ignite and possibly drive a burning front into the carbon and oxygen fuel. This track to thermonuclear explosions of white dwarfs was first discussed by Whelan & Iben (1973), Nomoto (1982a), Iben & Tutukov (1984) and Paczynski (1985). The major problem of these models has always been that nearly all possible accretion rates can be ruled out by strong arguments (Nomoto 1982a, Munari & Renzini 1992, Cassisi et al 1996, Tutukov & Yungelson 1996, Livio et al 1996, King & Van Teeseling 1998, Kato & Hachisu 1999, Cassisi et al 1998). In short, it is believed that white dwarfs accreting hydrogen at a low rate undergo nova eruptions and lose more mass in the outburst than they have accreted prior to it (e.g. Beer 1974, Gehrz et al 1993). At moderate accretion rates, a degenerate layer of helium is thought to form which might flash and could give rise to sub-Chandrasekhar explosions (which have other problems, as is discussed later). Next, still higher accretion rates can lead to quiet hydrostatic burning of H and He, but these systems should be so bright that they could easily be detected. However, it is not clear beyond doubt that they coincide with any of the known symbiotic or cataclysmic binaries. Very high accretion rates, finally, would form an extended H-rich red giant envelope around the white dwarf with debris not seen in the explosions (Nomoto et al 1979) (see also Figure 2). Therefore, it is uncertain whether white dwarfs accreting hydrogen from a companion star can ever reach the M_{chan} (Cassisi et al 1998).

Some of these arguments may be questioned, however. Firstly, a class of binary systems has recently been discovered, the so-called Supersoft X-ray Sources, which are best interpreted as white dwarfs accreting hydrogen-rich matter at such a high rate that H burns steadily (Truemper et al 1991, Greiner et al 1991, Van Den Heuvel et al 1992, Southwell et al 1996, Kahabka & Van den Heuvel 1997). It appears that if these white dwarfs could retain the accreted gas, they might be good candidates for SN Ia progenitors. In principle, they could accrete a few tenths of a solar mass with a typical accretion rate of a few $10^{-7} M_{\odot}/\text{year}$ over the estimated lifetime of such systems of several 10^9 years. Because most of them are heavily extinct, their total number might be sufficiently high (Di Stefano & Rappaport 1994; see also Livio 1996, Yungelson et al 1996), although this statement is certainly model dependent. However, some of the Supersoft X-ray Sources are known to be

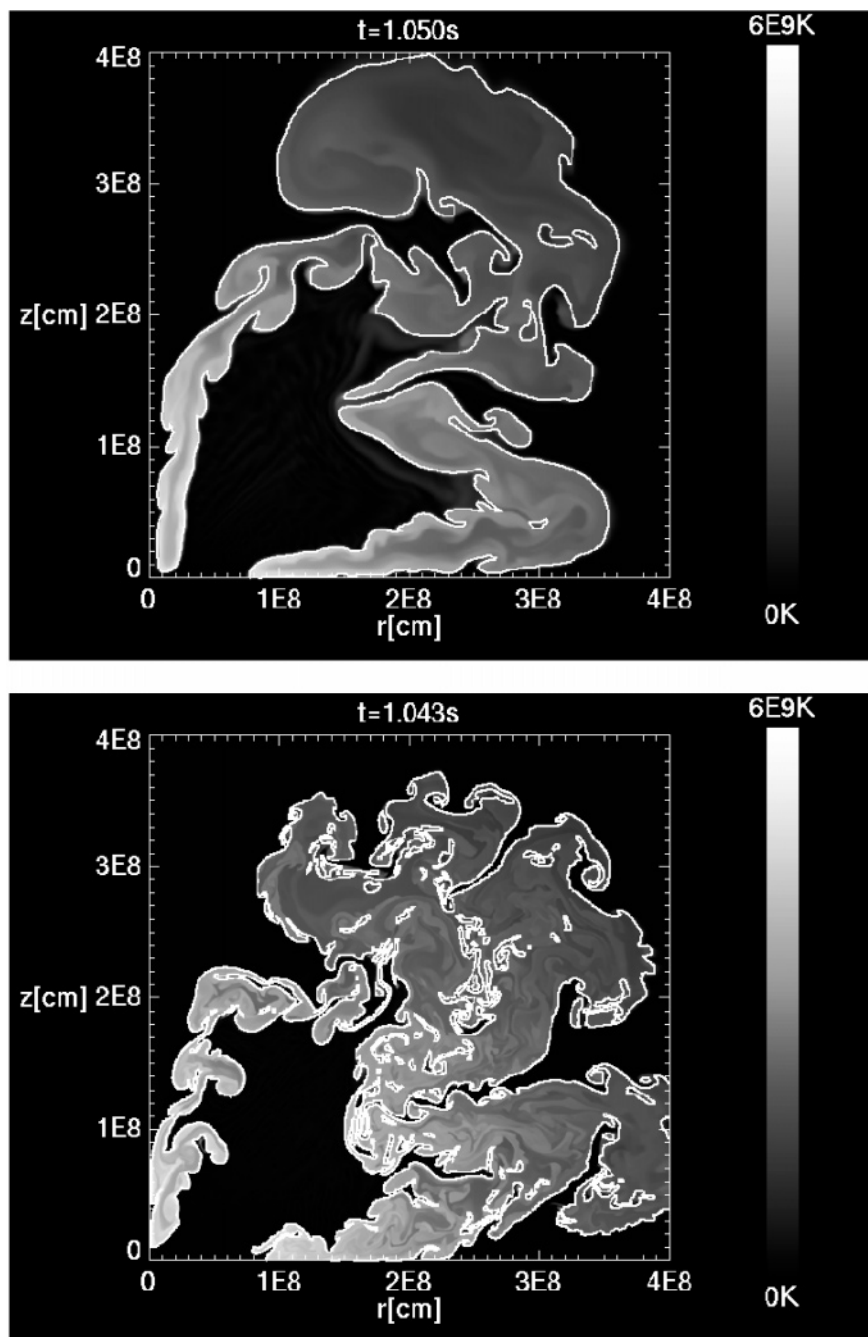


Figure 3 Snapshots of the temperature and the front geometry in a Chandrasekhar-mass deflagration model at 1.05 s (from Reinecke et al, 1999c). Shown are a model with "low" resolution (256^2) (upper figure) and one with three times higher resolution, respectively. Because of the larger surface area of the better-resolved model, it exploded, whereas the other one remained marginally bound.

variable in X-rays (but not in the optical wave bands) on timescales of weeks (Pakull et al 1993), too short to be related with the H-burning shell, possibly indicating substantial changes in the accretion rates. It therefore may not be justified to assume that the accretion rates we see now are sustained over several 10^9 years. But their very existence provides a first and strong case for the single-degenerate scenario.

Secondly, the minimum accretion rate at which hydrogen burns quietly without a nova outburst is uncertain. All models that compute this rate ignore important pieces of physics, and therefore, their predictions could be off by orders of magnitude. For example, classical nova outbursts require that the accreted hydrogen-rich envelope of the white dwarf also be heavily enriched in C and O from the white dwarf's core (see, e.g., Starrfield et al 1972, 1978; Sparks et al 1976; Truran 1982). One possible explanation has been that convective mixing and dredge-up might happen during the thermonuclear runaway, but recent numerical simulations indicate that this mechanism is insufficient (Kercek et al 1999). In contrast to spherically symmetric models, their three-dimensional (3D) simulations lead to a phase of quiet H-burning for accretion rates as low as $5 \times 10^{-9} M_{\odot}/\text{year}$ for a white dwarf of $1 M_{\odot}$ rather than a nova outburst with mass loss from the core. Other shortcomings include the assumption of spherical accretion with zero entropy, the neglect of magnetic fields, etc. So the dividing line between steady hydrogen burning and nova eruptions might leave some room for SN Ia progenitors.

Finally, it has been argued that the interaction of a wind from the white dwarf with the accretion flow from lobe-filling, low-mass red giant may open a wider path to type Ia supernovae. In a series of papers Hachisu et al (1996, 1999a, 1999b) discuss the effect that when the mass accretion rate exceeds a certain critical value, the envelope solution on the white dwarf is no longer static but corresponds to a strong wind. The strong wind stabilizes the mass transfer and limits the accretion rate in such a way that wind-loss rates and accretion rates become nearly equal. Consequently, the radius of the white dwarf does not increase with time and accretion rates leading to SNe Ia seem to be possible. However, their model assumes spherical accretion onto and a spherical wind from the white dwarf, which seem to be contradicting assumptions. But the idea should certainly be followed up.

4.3 Evolution to Ignition

In what follows, we assume most of the time that SN Ia progenitors are Chandrasekhar-mass C + O white dwarfs because, as discussed in the previous sections, this class of models seems to fit best the “typical” or “average” type Ia. In this subsection also, we do not discuss models in which two degenerate white dwarfs merge and form a critical mass for the ignition of carbon, mainly because the merging process will, in reality, be complex, and it is difficult to construct realistic explosion models (although with increasing computational resources it may be possible in the future).

But even if we consider only Chandrasekhar-mass white dwarfs as progenitor candidates, the information that is needed in order to model the explosion cannot be

obtained easily. In particular, the thermal structure and the chemical composition are uncertain. The C/O-ratio, for example, has to be known throughout the white dwarf, but this ratio depends on the main sequence mass of its progenitor and the metallicity of the gas from which it formed (Umeda et al 1999, Wellstein & Langer 1999). It was found that, depending on the main sequence mass, the central C/O can vary from 0.4 to 0.6, considerably less than assumed in most supernova models.

Next, the thermal structure of a white dwarf on its way to an explosion depends on the (convective) URCA process (Paczynski 1973; Iben 1978, 1982; Barkat & Wheeler 1990; Mochkovitch 1996). The URCA pairs $A = 21, 23$, and 25 (such as, e.g., $^{21}\text{Ne} / ^{21}\text{F}$, ...) can lead to either heating or cooling, and possibly even to a temperature inversion near the center of the white dwarf. The abundances of the URCA pairs depends again on the initial metallicity, which could, thus, affect the thermal structure of the white dwarf. Unfortunately, the convection in the degenerate star is likely to be nonlocal, time-dependent, 3D, and subsonic, but it needs to be modeled over very long (secular) timescales. It is not likely that in the near future we will be able to model these processes in a realistic manner, even on supercomputers.

Because of these difficulties, numerical studies of the explosion rely on ad hoc assumptions fixing the initial conditions, which are usually chosen to be as simple as possible. Realistic simulations have to be multidimensional, as is explained in the next section, and therefore numerical studies can only investigate a small fraction of the available parameter space. The failure or success of a particular model to explain certain observational results may, therefore, not be conclusive.

5. EXPLOSION MODELING

Numerical models are needed to provide the density, temperature, composition, and velocity fields of the supernova ejecta that result from the thermonuclear explosion of a white dwarf, accepted by most researchers as the “standard model” for SNe Ia (Sections 2, 4). This information can then be used to compute the resulting light curve and spectra with the help of radiation transport codes (Section 3) or to compare the relative distribution of isotopes with the observed solar abundances.

To a very good approximation, the exploding white dwarf material can be described as a fully ionized plasma with varying degrees of electron degeneracy, satisfying the fluid approximation. The governing equations are the hydrodynamical equations for mass, species, momentum, and energy transport, including gravitational acceleration, viscosity, heat and mass diffusion (Landau & Lifshitz 1995), and nuclear energy generation (Arnett 1996). They must be supplemented by an equation of state for an ideal gas of nuclei, an arbitrarily relativistic and degenerate electron gas, radiation, and electron-positron pair production and annihilation (Cox & Giuli 1968). The gravitational potential is calculated with the help of the Poisson equation. In numerical simulations that fully resolve the relevant length scales for dissipation, diffusion, and nuclear burning, it is possible to obtain the

energy generation rate from a nuclear reaction network (for a recent overview, see Timmes 1999) and the diffusion coefficients from an evaluation of the kinetic transport mechanisms (Nandkumar & Pethick 1984). If, on the other hand, these scales are unresolved—as is usually the case in simulations on scales of the stellar radius—subgrid-scale models are required to compute (or parameterize) the effective large-scale transport coefficients and burning rates, which are more or less unrelated to the respective microphysical quantities (Khokhlov 1995, Niemeyer & Hillebrandt 1995b).

Initial conditions can be obtained from hydrostatic spherically symmetric models of the accreting white dwarf or—for Chandrasekhar mass progenitors—from the Chandrasekhar equation for a fully degenerate, zero-temperature white dwarf (Kippenhahn & Weigert 1989). Given the initial conditions and symmetries specifying the boundary conditions, the dynamics of the explosion can in principle be determined by numerically integrating the equations of motion. Müller (1998) gives a detailed account of some current numerical techniques used for modeling supernovae.

Until the mid-1990s, most work on SN Ia explosions was done studying 1D, spherically symmetric models. This approach inherently lacks some important aspects of multidimensional thermonuclear burning relevant for M_{chan} -explosion models, e.g. off-center flame ignition, flame instabilities, and turbulence, which have to be mimicked by means of a spherical flame front with an undetermined turbulent flame speed, e.g. Nomoto et al (1976, 1984), Woosley & Weaver (1986a), Woosley (1990). In spite of these caveats, 1D models still represent the only reasonable approach to combine the hydrodynamics with detailed nucleosynthesis calculations and to carry out parameter studies of explosion scenarios. In fact, most of the phenomenology of SN Ia explosions and virtually all of the model predictions for spectra and light curves are based on spherically symmetric models. Several recent articles (Woosley 1990, Nomoto et al 1996, Hoefflich & Khokhlov 1996, Iwamoto et al 1999) describe the methodology and trends observed in these studies, as well as their implications regarding the cosmological supernova surveys (Hoefflich et al 1998b, Ruiz-Lapuente & Canal 1998, Umeda et al 1999, Sorokina et al 1999).

Following the pioneering work of Müller & Arnett (1982, 1986), some groups have explored the dynamics of 2D (Livne 1993; Arnett & Livne 1994a,b; Niemeyer & Hillebrandt 1995b; Niemeyer et al 1996; Arnett 1997; Reinecke et al 1999a) and 3D (Khokhlov 1994, 1995; Bravo & Garcia-Senz 1997; Benz 1997) explosion models, triggering the development of numerical algorithms for representing thin propagating surfaces in large-scale simulations (Khokhlov 1993a, Niemeyer & Hillebrandt 1995b, Bravo & Garcia-Senz 1995, Arnett 1997, Garcia-Senz et al 1998, Reinecke et al 1999b). It has also become possible to perform 2D and 3D direct numerical simulations, i.e. fully resolving the relevant burning and diffusion scales, of microscopic flame instabilities and flame-turbulence interactions (Niemeyer & Hillebrandt 1995a, Khokhlov 1995, Niemeyer & Hillebrandt 1997, Niemeyer et al 1999).

5.1 Chandrasekhar Mass Explosion Models

Given the overall homogeneity of SNe Ia (Section 2.1), the good agreement of parameterized 1D M_{chan} models with observed spectra and light curves, and their reasonable nucleosynthetic yields, the bulk of normal SNe Ia is generally assumed to consist of exploding M_{chan} C + O white dwarfs (Hoyle & Fowler 1960, Arnett 1969, Hansen & Wheeler 1969). In spite of three decades of work on the hydrodynamics of this explosion mechanism (beginning with Arnett (1969)), no clear consensus has been reached as to whether the star explodes as a result of a subsonic nuclear deflagration that becomes strongly turbulent (Ivanova et al 1974; Buchler & Mazurek 1975; Nomoto et al 1976, 1984; Woosley et al 1984), or whether this turbulent flame phase is followed by a delayed detonation during the expansion (Khokhlov 1991a,b; Woosley & Weaver 1994a) or after one or many pulses (Khokhlov 1991b; Arnett & Livne 1994a,b). Only the prompt detonation mechanism is agreed to be inconsistent with SN Ia spectra, as it fails to produce sufficient amounts of intermediate mass elements (Arnett 1969, Arnett et al 1971).

This apparently slow progress is essentially a consequence of the overwhelming complexity of turbulent flame physics and deflagration-detonation transitions (DDTs) (Williams 1985, Zeldovich et al 1985) that makes first-principle predictions based on M_{chan} explosion models nearly impossible. The existence of an initial subsonic flame phase is, it seems, an unavoidable ingredient of all M_{chan} models (and only those) where it is required to preexpand the stellar material prior to its nuclear consumption in order to avoid the almost exclusive production of iron-peaked nuclei (Nomoto et al 1976, 1984; Woosley & Weaver 1986a).

Guided by parameterized 1D models that yield estimates for the values for the turbulent flame speed S_t and the DDT transition density ρ_{DDT} (e.g. Hoefflich & Khokhlov 1996), much work has been done recently on the physics of buoyancy-driven, turbulent thermonuclear flames in exploding M_{chan} white dwarfs. The close analogy with thin chemical premixed flames has been exploited to develop a conceptual framework that covers all scales from the white dwarf radius to the microscopic flame thickness and dissipation scales (Khokhlov 1995, Niemeyer & Woosley 1997). In the following discussions of nuclear combustion, flame ignition, and the various scenarios for M_{chan} explosions characterized by the sequence of combustion modes, we emphasize the current understanding of physical processes rather than empirical fits of light curves and spectra.

5.1.1 Flames, Turbulence, and Detonations Owing to the strong temperature dependence of the nuclear reaction rates, $\dot{S} \sim T^{12}$ at $T \approx 10^{10}$ K (Hansen & Kawaler 1994:247), nuclear burning during the explosion is confined to microscopically thin layers that propagate either conductively as subsonic deflagrations (“flames”) or by shock compression as supersonic detonations (Courant & Friedrichs 1948, Landau & Lifshitz 1995:Ch. 14). Both modes are hydrodynamically unstable to spatial perturbations, as can be shown by linear perturbation analysis. In the nonlinear regime, the burning fronts either are stabilized by forming

a cellular structure or become fully turbulent—either way, the total burning rate increases as a result of flame surface growth (Lewis & von Elbe 1961, Williams 1985, Zeldovich et al 1985). Neither flames nor detonations can be resolved in explosion simulations on stellar scales and therefore must be represented by numerical models.

When the fuel exceeds a critical temperature T_c where burning proceeds nearly instantaneously compared with the fluid motions [for a suitable definition of T_c , see Timmes & Woosley (1992)], a thin reaction zone forms at the interface between burned and unburned material. It propagates into the surrounding fuel by one of two mechanisms allowed by the Rankine-Hugoniot jump conditions: a deflagration (“flame”) or a detonation (cf Figure 2.5 in Williams 1985).

If the overpressure created by the heat of the burning products is sufficiently high, a hydrodynamical shock wave forms that ignites the fuel by compressional heating. A self-sustaining combustion front that propagates by shock heating is called a detonation. Detonations generally move supersonically and therefore do not allow the unburned medium to expand before it is burned. Their speed depends mainly on the total amount of energy released per unit mass, ϵ , and is therefore more robustly computable than deflagration velocities. A good estimate for the velocity of planar strong detonations is the Chapman-Jouget velocity (Lewis & von Elbe 1961, Zeldovich et al 1985, Williams 1985, and references therein). The nucleosynthesis, speed, structure, and stability of planar detonations in degenerate C + O material was analyzed by Imshennik & Khokhlov (1984), by Khokhlov (1988, 1989, 1993b), and recently by Kriminski et al (1998) and Imshennik et al (1999), who claim that C + O detonations are one-dimensionally unstable and therefore cannot occur in exploding white dwarfs above a critical density of $\sim 2 \times 10^7 \text{ g cm}^{-3}$ (Kriminski et al 1998) (cf Section 5.1.3).

If, on the other hand, the initial overpressure is too weak, the temperature gradient at the fuel-ashes interface steepens until an equilibrium between heat diffusion (carried out predominantly by electron-ion collisions) and energy generation is reached. The resulting combustion front consists of a diffusion zone that heats up the fuel to T_c , followed by a thin reaction layer where the fuel is consumed and energy is generated. It is called a deflagration or simply a flame and moves subsonically with respect to the unburned material (Landau & Lifshitz 1995). Flames, unlike detonations, may therefore be strongly affected by turbulent velocity fluctuations of the fuel. Only if the unburned material is at rest, a unique laminar flame speed S_1 can be found, which depends on the detailed interaction of burning and diffusion within the flame region (e.g. Zeldovich et al 1985). According to Landau & Lifshitz (1995), it can be estimated by assuming that in order for burning and diffusion to be in equilibrium, the respective timescale timescales, $\tau_b \sim \epsilon/\dot{w}$ and $\tau_d \sim \delta^2/\kappa$, where δ is the flame thickness and κ is the thermal diffusivity, must be similar: $\tau_b \sim \tau_d$. Defining $S_1 = \delta/\tau_b$, one finds $S_1 \sim (\kappa \dot{w}/\epsilon)^{1/2}$, where \dot{w} should be evaluated at $T \approx T_c$ (Timmes & Woosley 1992). This is only a crude estimate due to the strong T dependence of \dot{w} . Numerical solutions of the full equations of hydrodynamics, including

nuclear energy generation and heat diffusion, are needed to obtain more accurate values for S_1 as a function of ρ and fuel composition. Laminar thermonuclear carbon and oxygen flames at high to intermediate densities were investigated by Buchler et al (1980), Ivanova et al (1982), and Woosley & Weaver (1986b), and, using a variety of different techniques and nuclear networks, by Timmes & Woosley (1992). For the purpose of SN Ia explosion modeling, one needs to know the laminar flame speed $S_1 \approx 10^7 \dots 10^4 \text{ cm s}^{-1}$ for $\rho \approx 10^9 \dots 10^7 \text{ g cm}^{-3}$, the flame thickness $\delta = 10^{-4} \dots 1 \text{ cm}$ (defined here as the width of the thermal preheating layer ahead of the much thinner reaction front), and the density contrast between burned and unburned material $\mu = \Delta\rho/\rho = 0.2 \dots 0.5$ [all values quoted here assume a composition of $X_C = X_O = 0.5$, (Timmes & Woosley 1992)]. The thermal expansion parameter μ reflects the partial lifting of electron degeneracy in the burning products and is much lower than the typical value found in chemical, ideal gas systems (Williams 1985).

Observed on scales much larger than δ , the internal reaction-diffusion structure can be neglected and the flame can be approximated as a density jump that propagates locally with the normal speed S_1 . This “thin flame” approximation allows a linear stability analysis of the front with respect to spatial perturbations. The result shows that thin flames are linearly unstable on all wavelengths. It was discovered first by Landau (1944) and Darrieus (1944), and is hence called the Landau-Darrieus (LD) instability. Subject to the LD instability, perturbations grow until a web of cellular structures forms and stabilizes the front at finite perturbation amplitudes (Zeldovich 1966). The LD instability therefore does not, in general, lead to the production of turbulence. In the context of SN Ia models, the nonlinear LD instability was studied by Blinnikov & Sasorov (1996), using a statistical approach based on the Frankel equation, and by Niemeyer & Hillebrandt (1995a) employing 2D hydrodynamics and a one-step burning rate. Both groups concluded that the cellular stabilization mechanism precludes a strong acceleration of the burning front as a result of the LD instability. However, Blinnikov & Sasorov (1996) mention the possible breakdown of stabilization at low stellar densities (i.e. high μ), which is also indicated by the lowest density run of Niemeyer & Hillebrandt (1995a)—this may be important in the framework of active turbulent combustion (see below). The linear growth rate of LD unstable thermonuclear flames with arbitrary equation of state was derived by Bychkov & Liberman (1995a). The same authors also found a 1D, pulsational instability of degenerate C + O flames (Bychkov & Liberman 1995b), which was later disputed by Blinnikov (1996).

The best-studied and probably most important hydrodynamical effect for modeling SN Ia explosions is the Rayleigh-Taylor (RT) instability (Rayleigh 1883, Chandrasekhar 1961) resulting from the buoyancy of hot, burned fluid with respect to the dense, unburned material. Several groups have investigated the RT instability of nuclear flames in SNe Ia by means of numerical hydrodynamical simulations (Müller & Arnett 1982, 1986; Livne 1993; Khokhlov 1994, 1995; Niemeyer & Hillebrandt 1995b). After more than five decades of experimental and numerical

work, the basic phenomenology of nonlinear RT mixing is fairly well understood (Fermi 1951, Layzer 1955, Sharp 1984, Read 1984, Youngs 1984): Subject to the RT instability, small surface perturbations grow until they form bubbles (or “mushrooms”) that begin to float upward while spikes of dense fluid fall down. In the nonlinear regime, bubbles of various sizes interact and create a foamy RT mixing layer whose vertical extent h_{RT} grows with time t according to a self-similar growth law, $h_{\text{RT}} = \alpha g(\mu/2)t^2$, where α is a dimensionless constant ($\alpha \approx 0.05$) and g is the background gravitational acceleration (Sharp 1984, Youngs 1984, Read 1984).

Secondary instabilities related to the velocity shear along the bubble surfaces (Niemeyer & Hillebrandt 1997) quickly lead to the production of turbulent velocity fluctuations that cascade from the size of the largest bubbles ($\approx 10^7$ cm) down to the microscopic Kolmogorov scale, $l_k \approx 10^{-4}$ cm, where they are dissipated (Niemeyer & Hillebrandt 1995b, Khokhlov 1995). Because no computer is capable of resolving this range of scales, one must resort to statistical or scaling approximations of those length scales that are not properly resolved. The most prominent scaling relation in turbulence research is Kolmogorov’s law for the cascade of velocity fluctuations, stating that in the case of isotropy and statistical stationarity, the mean velocity v of turbulent eddies with size l scales as $v \sim l^{1/3}$ (Kolmogorov 1941). Knowledge of the eddy velocity as a function of length scale is important to classify the burning regime of the turbulent combustion front (Niemeyer & Woosley 1997, Niemeyer & Kerstein 1997, Khokhlov et al 1997). The ratio of the laminar flame speed and the turbulent velocity on the scale of the flame thickness, $K = S_l/v(\delta)$, plays an important role: If $K \gg 1$, the laminar flame structure is nearly unaffected by turbulent fluctuations. Turbulence does, however, wrinkle and deform the flame on scales l , where $S_l \ll v(l)$, i.e. above the Gibson scale l_g defined by $S_l = v(l_g)$ (Peters 1988). These wrinkles increase the flame surface area and therefore the total energy generation rate of the turbulent front (Damköhler 1940). In other words, the turbulent flame speed, S_t , defined as the mean overall propagation velocity of the turbulent flame front, becomes larger than the laminar speed S_l . If the turbulence is sufficiently strong, $v(L) \gg S_l$, the turbulent flame speed becomes independent of the laminar speed, and therefore of the microphysics of burning and diffusion, and scales only with the velocity of the largest turbulent eddy (Damköhler 1940, Clavin 1994):

$$S_t \sim v(L). \quad (2)$$

Because of the unperturbed laminar flame properties on very small scales, and the wrinkling of the flame on large scales, the burning regime where $K \gg 1$ is called the corrugated flamelet regime (Pope 1987, Clavin 1994).

As the density of the white dwarf material declines and the laminar flamelets become slower and thicker, it is plausible that at some point turbulence significantly alters the thermal flame structure (Khokhlov et al 1997, Niemeyer & Woosley 1997). This marks the end of the flamelet regime and the beginning of the distributed burning, or distributed reaction zone, regime (e.g. Pope 1987). So far,

modeling the distributed burning regime in exploding white dwarfs has not been attempted explicitly because neither nuclear burning and diffusion nor turbulent mixing can be properly described by simplified prescriptions. Phenomenologically, the laminar flame structure is believed to be disrupted by turbulence and to form a distribution of reaction zones with various lengths and thicknesses. In order to find the critical density for the transition between both regimes, we need to formulate a specific criterion for flamelet breakdown. A criterion for the transition between both regimes is discussed by Niemeyer & Woosley (1997), Niemeyer & Kerstein (1997) and Khokhlov et al (1997):

$$l_{\text{cutoff}} \leq \delta. \quad (3)$$

Inserting the results of Timmes & Woosley (1992) for S_l and δ as functions of density, and using a typical turbulence velocity $v(10^6 \text{ cm}) \sim 10^7 \text{ cm s}^{-1}$, the transition from flamelet to distributed burning can be shown to occur at a density of $\rho_{\text{dis}} \approx 10^7 \text{ g cm}^{-3}$ (Niemeyer & Kerstein 1997).

The close coincidence of ρ_{dis} and the preferred value for ρ_{DDT} (Hoeftlich & Khokhlov 1996, Nomoto et al 1996) inspired some authors (Niemeyer & Woosley 1997, Khokhlov et al 1997) to suggest that both are related by local flame quenching and reignition via the Zeldovich induction time gradient mechanism (Zeldovich et al 1970), whereby a macroscopic region with a uniform temperature gradient can give birth to a supersonic spontaneous combustion wave that steepens into a detonation (Woosley 1990, and references therein). In the context of the SN Ia explosion mechanism, this effect was first analyzed by Blinnikov & Khokhlov (1986, 1987). Whether or not the gradient mechanism can account for DDTs in the delayed detonation scenario for SNe Ia is still controversial: Khokhlov et al (1997) conclude that it can, whereas Niemeyer (1999)—using arguments based on incompressible computations of microscopic flame-turbulence interactions by Niemeyer et al (1999)—states that thermonuclear flames may be too robust with respect to turbulent quenching to allow the formation of a sufficiently uniform temperature gradient.

Assuming that the nonlinear RT instability dominates the turbulent flow that advects the flame, the passive-surface description of the flame neglects the additional stirring caused by thermal expansion within the flame brush itself, accelerating the burnt material in random directions. Both the spectrum and cutoff scale may be affected by “active” turbulent combustion (Kerstein 1996, Niemeyer & Woosley 1997). Although the small expansion coefficient μ indicates that the effect is weak compared with chemical flames, a quantitative answer is still missing.

Finally, we note that some authors also studied the multidimensional instability of detonations in degenerate C + O matter (Boisseau et al 1996, Gamezo et al 1999), finding unsteady front propagation, the formation of a cellular front structure, and locally incomplete burning in multidimensional C + O detonations. These effects may have interesting implications for SN Ia scenarios involving a detonation phase.

5.1.2 Flame Ignition As the white dwarf grows close to the Chandrasekhar mass $M_{\text{chan}} \approx 1.4M_{\odot}$, the energy budget near the core is governed by plasmon neutrino losses and compressional heating. The neutrino losses increase with growing central density until the latter reaches approximately $2 \times 10^9 \text{ g cm}^{-3}$ (Woosley & Weaver 1986a). At this point, plasmon creation becomes strongly suppressed while electron screening of nuclear reactions enhances the energy generation rate until it begins to exceed the neutrino losses. This “smoldering” of the core region marks the beginning of the thermonuclear runaway (Arnett 1969, 1971; Woosley & Weaver 1986a). During the following ~ 1000 years, the core experiences internally heated convection with progressively smaller turnover timescales τ_c . Simultaneously, the typical timescale for thermonuclear burning, τ_b , drops even faster as a result of the rising core temperature and the steep temperature dependence of the nuclear reaction rates.

During this period, the entropy and temperature evolution of the core is affected by the convective URCA process, a convectively driven electron capture-beta decay cycle leading to neutrino-antineutrino losses. It was first described in this context by Paczynski (1972), who argued it would cause net cooling and therefore delay the runaway. Since then, the convective URCA process was revisited by several authors (e.g. Bruenn 1973, Iben 1982, Barkat & Wheeler 1990, Mochkovitch 1996), who alternately claimed that it results in overall heating or cooling. The most recent analysis (Stein et al 1999) concludes that although the URCA neutrinos carry away energy, they cannot cool the core globally but instead slow down the convective motions.

At $T \approx 7 \times 10^8 \text{ K}$, τ_c and τ_b become comparable, indicating that convective plumes burn at the same rate as they circulate (Nomoto et al 1984, Woosley & Weaver 1986a). Experimental or numerical data describing this regime of strong reactive convection is not available, but several groups are planning to conduct numerical experiments at the time this article is written. At $T \approx 1.5 \times 10^9 \text{ K}$, τ_b becomes extremely small compared with τ_c , and carbon and oxygen virtually burn in place. A new equilibrium between energy generation and transport is found on much smaller length scales, $l \approx 10^{-4} \text{ cm}$, where thermal conduction by degenerate electrons balances nuclear energy input (Timmes & Woosley 1992). The flame is born.

The evolution of the runaway immediately prior to ignition of the flame is crucial for determining its initial location and shape. Using a simple toy model, Garcia-Senz & Woosley (1995) found that under certain conditions, burning bubbles subject to buoyancy and drag forces can rise a few hundred kilometers before flame formation, which suggests a high probability for off-center ignition at multiple, unconnected points. As a consequence, more material burns at lower densities, thus producing higher amounts of intermediate mass elements than a centrally ignited explosion. In a parameter study, Niemeyer et al (1996) and Reinecke et al (1999a) demonstrated the significant influence of the location and number of initially ignited spots on the final explosion energetics and nucleosynthesis.

5.1.3 Prompt Detonation The first hydrodynamical simulation of an exploding M_{chan} white dwarf (Arnett 1969) assumed that the thermonuclear combustion commences as a detonation wave, consuming the entire star at the speed of sound. Given no time to expand prior to being burned, the C + O material in this scenario is transformed almost completely into iron-peak nuclei and thus fails to produce significant amounts of intermediate mass elements, in contradiction to observations (Filippenko 1997a,b). It is for this reason that prompt detonations are generally considered ruled out as viable candidates for the SN Ia explosion mechanism.

In addition to the empirical evidence, the ignition of a detonation in the high-density medium of the white dwarf core was argued to be an unlikely event. In spite of the smallness of the critical mass for detonation at $\rho \approx 2 \times 10^9 \text{ g cm}^{-3}$ (Niemeyer & Woosley 1997, Khokhlov et al 1997) and the correspondingly large number of critical volumes in the core ($\sim 10^{18}$), the stringent uniformity condition for the temperature gradient of the runaway region (Blinnikov & Khokhlov 1986, 1987) was shown to be violated even by the minute amounts of heat dissipated by convective motions (Niemeyer & Woosley 1997). A different argument against the occurrence of a prompt detonation in C + O white dwarf cores was given by Krinski et al (1998), who found that C + O detonations may be subject to self-quenching at high material densities ($\rho > 2 \times 10^7 \text{ g cm}^{-3}$) (see also Imshennik et al 1999).

5.1.4 Pure Turbulent Deflagration Once ignited (Section 5.1.2), the subsonic thermonuclear flame becomes highly convoluted as a result of turbulence produced by the various flame instabilities (Section 5.1.1). It continues to burn through the star until it either transitions into a detonation or is quenched by expansion. The key questions with regard to explosion modeling are the following: (a) What is the effective turbulent flame speed S_t as a function of time, (b) is the total amount of energy released during the deflagration phase enough to unbind the star and produce a healthy explosion, and (c) does the resulting ejecta composition and velocity agree with observations?

By far the most work has been done on 1D models, ignoring the multidimensionality of the flame physics and instead parameterizing S_t in order to answer the second and third questions (for reviews, see Woosley & Weaver 1986a, Nomoto et al 1996). One of the most successful examples, model W7 of Nomoto et al (1984), clearly demonstrates the excellent agreement of “fast” deflagration models with SN Ia spectra and light curves. S_t has been parameterized differently by different authors, for instance as a constant fraction of the local sound speed (Hoeftlich & Khokhlov 1996, Iwamoto et al 1999), using time-dependent convection theory (Nomoto et al 1976, 1984; Buchler & Mazurek 1975; Woosley et al 1984), or with a phenomenological fractal model describing the multiscale character of the wrinkled flame surface (Woosley 1990, 1997b). All these studies essentially agree that very good agreement with the observations is obtained if S_t accelerates up to roughly 30% of the sound speed. There remains a problem with

the overproduction of neutron-rich iron-group isotopes in fast deflagration models (Woosley et al 1984, Thielemann et al 1986, Iwamoto et al 1999), but this may be alleviated in multiple dimensions (see below). Turning this argument around, Woosley (1997a) argues that ^{48}Ca can only be produced by carbon burning in the very-high-density regime of a M_{chan} white dwarf core, providing a clue that a few SNe Ia need to be M_{chan} explosions igniting at $\rho \geq 2 \times 10^9 \text{ g cm}^{-3}$. A slightly different approach to 1D SN Ia modeling was taken by Niemeyer & Woosley (1997), who employed the self-similar growth rate of RT mixing regions (Section 5.1.1) to prescribe the turbulent flame speed. Here, all the free parameters are fixed by independent simulations or experiments. The result shows a successful explosion, albeit short on intermediate mass elements, which suggests that the employed flame model is still too simplistic.

A number of authors have studied multidimensional deflagrations in exploding M_{chan} white dwarfs using a variety of hydrodynamical methods (Livne 1993, Arnett & Livne 1994a, Khokhlov 1995, Niemeyer & Hillebrandt 1995b, Niemeyer et al 1996, Reinecke et al 1999a). The problem of simulating subsonic flames in large-scale simulations has two aspects: the representation of the thin, propagating surface separating hot and cold material with different densities, and the prescription of the local propagation velocity $S_t(\Delta)$ of this surface as a function of the hydrodynamical state of the large-scale calculation with numerical resolution Δ . The former problem has been addressed with artificial reaction-diffusion fronts in codes based on the Piecewise Parabolic Method (PPM) (Khokhlov 1995, Niemeyer & Hillebrandt 1995b, Niemeyer et al 1996) and Smoothed Particle Hydrodynamics (SPH) (Garcia-Senz et al 1998), in a PPM-specific flame-tracking technique (Arnett 1997), and in a hybrid flame-capturing/tracking method based on level sets (Reinecke et al 1999b) (see Figure 3, color insert). Regarding the flame speed prescription, some authors assigned the local front propagation velocity assuming that the flame is laminar on unresolved scales $l < \Delta$ (Arnett & Livne 1994a), by postulating that $S_t(\Delta)$ is dominated by the terminal rise velocity of Δ -sized bubbles (Khokhlov 1995), or by using Equation 2 together with a subgrid-scale model for the unresolved turbulent kinetic energy providing $v(\Delta)$ (Niemeyer & Hillebrandt 1995b, Niemeyer et al 1996, Reinecke et al 1999a).

In most multidimensional calculations on stellar scales to date, the effective turbulent flame speed stayed below the required 30% of the sound speed. The detailed outcome of the explosion is controversial: Whereas some calculations show that the star remains gravitationally bound after the deflagration phase has ceased (Khokhlov 1995), others indicate that S_t may be large enough to produce a weak but definitely unbound explosion (Niemeyer et al 1996). These discrepancies can probably be attributed to differences in the description of the turbulent flame and to numerical resolution effects that plague all multidimensional calculations.

Niemeyer & Woosley (1997) and Niemeyer (1999) speculate about additional physics that can increase the burning rate in turbulent deflagration models, in particular multipoint ignition and active turbulent combustion (ATC), i.e. the generation of additional turbulence by thermal expansion within the turbulent flame

brush. ATC can, in principle, explain the acceleration of S_t up to some fraction of the sound speed (Kerstein 1996), but its effectiveness is unknown. Multipoint ignition, on the other hand, has already been shown to significantly increase the total energy release compared with single-point ignition models (Niemeyer et al 1996, Reinecke et al 1999a). Furthermore, it allows more material to burn at lower densities, thus alleviating the nucleosynthesis problem of 1D fast deflagration models (Niemeyer et al 1996).

We conclude the discussion of the pure turbulent deflagration scenario with a checklist of the model requirements summarized in Section 2.4. Assuming that some combination of buoyancy, ATC, and multipoint ignition can drive the effective turbulent flame speed to $\sim 30\%$ of the sound speed—which is not evident from multidimensional simulations—one can conclude from 1D simulations that pure deflagration models readily comply with all observational constraints. Most authors agree that S_t decouples from microphysics on large enough scales and becomes dominated by essentially universal hydrodynamical effects, making the scenario intrinsically robust. A noteworthy exception is the location and number of ignition points that can strongly influence the explosion outcome and may be a possible candidate for the mechanism giving rise to the explosion strength variability. Other possible sources of variations include the ignition density and the accretion rate of the progenitor system (Umeda et al 1999, Iwamoto et al 1999). All these effects may potentially vary with composition and metallicity and can therefore account for the dependence on the progenitor stellar population.

5.1.5 Delayed Detonation Turbulent deflagrations can sometimes be observed to undergo spontaneous transitions to detonations [deflagration-detonation transitions (DDTs)] in terrestrial combustion experiments (e.g. Williams 1985:217–19). Thus inspired, it was suggested that DDTs may occur in the late phase of a M_{chan} explosion, providing an elegant explanation for the initial slow burning required to preexpand the star, followed by a fast combustion mode that produces large amounts of high-velocity intermediate mass elements (Khokhlov 1991a, Woosley & Weaver 1994a). Meanwhile, many 1D simulations have demonstrated the capability of the delayed detonation scenario to provide excellent fits to SN Ia spectra and light curves (Woosley 1990, Hoeflich & Khokhlov 1996), as well as reasonable nucleosynthesis products with regard to solar abundances (Khokhlov 1991b, Iwamoto et al 1999). In the best-fit models, the initial flame phase has a slow velocity of roughly 1% of the sound speed and transitions to detonation at a density of $\rho_{\text{DDT}} \approx 10^7 \text{ g cm}^{-3}$ (Hoeflich & Khokhlov 1996, Iwamoto et al 1999). The transition density was also found to be a convenient parameter to explain the observed sequence of explosion strengths (Hoeflich & Khokhlov 1996).

Various mechanisms for DDT were discussed in the early literature on delayed detonations (see Niemeyer & Woosley 1997, and references therein). Recent investigations have focussed on the induction time gradient mechanism (Zeldovich et al 1970, Lee et al 1978), analyzed in the context of SNe Ia by Blinnikov & Khokhlov (1986, 1987). It was realized by Khokhlov et al (1997) and Niemeyer

& Woosley (1997) that a necessary criterion for this mechanism is the local disruption of the flame sheet by turbulent eddies or, in other words, the transition of the burning regime from flamelet to distributed burning (Section 5.1.1). Simple estimates (Niemeyer & Kerstein 1997) show that this transition should occur at roughly 10^7 g cm^{-3} , providing a plausible explanation for the delay of the detonation.

The critical length (or mass) scale over which the temperature gradient must be held fixed in order to allow the spontaneous combustion wave to turn into a detonation was computed by Khokhlov et al (1997) and Niemeyer & Woosley (1997); it is a few orders of magnitude thicker than the final detonation front and depends very sensitively on composition and density.

The virtues of the delayed detonation scenario can again be summarized by completing the checklist of Section 2.4. It is undisputed that suitably tuned delayed detonations satisfy all the constraints given by SN Ia spectra, light curves, and nucleosynthesis. If ρ_{DDT} is indeed determined by the transition of burning regimes—which in turn might be composition dependent (Umeda et al 1999)—the scenario is also fairly robust and ρ_{DDT} may represent the explosion strength parameter. Note that in this case, the variability induced by multipoint ignition needs to be explained away. If, on the other hand, thermonuclear flames are confirmed to be almost unquenchable, the favorite mechanism for DDTs becomes questionable (Niemeyer 1999). Moreover, should the mechanism DDT rely on rare, strong turbulent fluctuations, one must ask about those events that fail to ignite a detonation following the slow deflagration phase, which, on its own, cannot give rise to a viable SN Ia explosion. They might end up as pulsational delayed detonations or as unobservably dim, as yet unclassified explosions. Multidimensional simulations of the turbulent flame phase may soon answer whether the turbulent flame speed is closer to 1% or 30% of the speed of sound and hence decide whether DDTs are a necessary ingredient of SN Ia explosion models.

5.1.6 Pulsational Delayed Detonation In this variety of the delayed detonation scenario, the first turbulent deflagration phase fails to release enough energy to unbind the star that subsequently pulses and triggers a detonation upon recollapse (Nomoto et al 1976; Khokhlov 1991b). This model was studied in 1D by Hoefflich & Khokhlov (1996) and Woosley (1997b) (who calls it “pulsed detonation of the first type”) and in 2D by Arnett & Livne (1994b). Hoefflich & Khokhlov (1996) report that it produces little ^{56}Ni but a substantial amount of Si and Ca and may therefore explain very subluminal events, such as SN 1991bg. Using a fractal flame parameterization, Woosley (1997b) also considered “pulsed deflagrations,” i.e. reignition occurs as a deflagration rather than a detonation, and “pulsed detonations of the second type,” in which the burning also reignites as a flame but later accelerates and touches off a detonation. This latter model closely resembles the standard delayed detonation, whereas the former may or may not produce a healthy explosion, depending on the prescribed speed of the rekindled flame (Woosley 1997b).

Obtaining a DDT by means of the gradient mechanism is considerably more plausible after one or several pulses than during the first expansion phase (Khokhlov et al 1997), as the laminar flame thickness becomes macroscopically large during the expansion, allowing the fuel to be preheated, and turbulence is significantly enhanced during the collapse.

The “checklist” for pulsational delayed detonations looks similar to that of simple delayed detonations (see above), with somewhat less emphasis on the improbability for DDT. Some fine-tuning of the initial flame speed is needed to obtain a large enough pulse in order to achieve a sufficient degree of mixing, while avoiding to unbind the star in a very weak explosion (Niemeyer & Woosley 1997). Again, these “fizzles” may be very subluminescent and may have escaped discovery. We finally note that all pulsational models are in conflict with multidimensional simulations that predict an unbound star after the first deflagration phase.

5.2 Sub-Chandrasekhar Mass Models

C + O white dwarfs below the Chandrasekhar mass do not reach the critical density and temperature for explosive carbon burning by accretion and therefore need to be ignited by an external trigger. Detonations in the accreted He layer were suggested to drive a strong enough shock into the C + O core to initiate a secondary carbon detonation (Weaver & Woosley 1980, Nomoto 1980, 1982b; Woosley et al 1980, Sutherland & Wheeler 1984, Iben & Tutukov 1984). The nucleosynthesis and light curves of sub- M_{chan} models, also known as helium ignitors or edge-lit detonations, were investigated in 1D (Woosley & Weaver 1994b, Hoefflich & Khokhlov 1996) and 2D (Livne & Arnett 1995) and found to be superficially consistent with SNe Ia, especially subluminescent ones (Ruiz-Lapuente et al 1993a). Their ejecta structure is characterized almost inevitably by an outer layer of high-velocity Ni and He above the intermediate-mass elements and the inner Fe/Ni core.

These models are favored mostly by the statistics of possible SN Ia progenitor systems (Yungelson & Livio 1998, Livio 1999) and by the straightforward explanation of the one-parameter strength sequence in terms of the white dwarf mass (Ruiz-Lapuente et al 1995). However, they appear to be severely challenged both photometrically and spectroscopically: Owing to the heating by radioactive ^{56}Ni in the outer layer, they are somewhat too blue at maximum brightness and their light curve rises and declines too steeply (Hoefflich & Khokhlov 1996, Nugent et al 1997, Hoefflich et al 1997). Perhaps even more stringent is the generic prediction of He ignitors to exhibit signatures of high-velocity Ni and He, rather than Si and Ca, in the early and maximum spectra, which is in strong disagreement with observations (Nugent et al 1997, Hoefflich et al 1997).

With respect to the explosion mechanism itself, the most crucial question is whether and where the He detonation manages to shock the C + O core sufficiently to create a carbon detonation. By virtue of their built-in spherical symmetry, 1D models robustly (and unphysically) predict a perfect convergence of the inward propagating pressure wave and subsequent carbon ignition near the core (Woosley

& Weaver 1994b). Some 2D simulations indicate that the C + O detonation is born off-center but still due to the convergence of the He-driven shock near the symmetry axis of the calculation (Livne 1990, Livne & Glasner 1991) whereas others find a direct initiation of the carbon detonation along the circle where the He detonation intersects the C + O core (Livne 1997, Arnett 1997, Wiggins & Falle 1997, Wiggins et al 1998). Using 3D SPH simulations, Benz (1997) failed to see carbon ignition in all but the highest-resolution calculations, where carbon was ignited directly at the interface rather than by shock convergence. Further, C ignition is facilitated if the He detonation starts at some distance above the interface, allowing the build-up of a fully developed pressure spike before it hits the carbon (Benz 1997). This result was confirmed by recent 3D SPH simulations (Garcia-Senz et al 1999) that also examined the effect of multiple He ignition points, finding enhanced production of intermediate mass elements in this case. Hence, multidimensional SPH and PPM simulations presently confirm the validity of He-driven carbon detonations, in particular by direct ignition, but they also demonstrate the need for very high numerical resolution in order to obtain mutually consistent results (Arnett 1997, Benz 1997).

To summarize, sub- M_{chan} models are most severely constrained by their prediction of an outer layer of high-velocity Ni and He. Should further research conclude that spectra, colors, and light curves are less contaminated by this layer than presently thought, they represent an attractive class of candidates for SNe Ia, especially subluminous ones, from the point of view of progenitor statistics and the one-parameter explosion strength family. Note, however, that the SN Ia luminosity function in this scenario is directly linked to the distribution of white dwarf masses, predicting a more gradual decline on the bright side of the luminosity function than indicated by observations (Vaughan et al 1995, Livio 1999). The explosion mechanism itself appears realistic, at least in the direct carbon ignition mode, but more work is needed to firmly establish the conditions for ignition of the secondary carbon detonation.

5.3 Merging White Dwarfs

The most obvious strength of the merging white dwarfs, or double-degenerate, scenario for SNe Ia (Webbink 1984, Iben & Tutukov 1984, Paczynski 1985) is the natural explanation for the lack of hydrogen in SN Ia spectra (Livio 1999) (cf Section 2.1). Furthermore, in contrast to the elusive progenitor systems for single-degenerate scenarios, there is some evidence for the existence of double-degenerate binary systems (Saffer et al 1998) despite earlier suspicions to the contrary (e.g. Bragaglia 1997). These systems are bound to merge as a consequence of gravitational wave emission with about the right statistics (Livio 1999) and give rise to some extreme astrophysical event, albeit not necessarily a SN Ia.

Spherically symmetric models of detonating merged systems, parameterized as C + O white dwarfs with thick envelopes, were analyzed by Hoefflich et al (1992), Khokhlov et al (1993) and Hoefflich & Khokhlov (1996), giving reasonable

agreement with SN Ia light curves. SPH simulations (3D) of white dwarfs mergers (Benz et al 1990, Rasio & Shapiro 1995, Mochkovitch et al 1997) show the disruption of the less-massive star in a matter of a few orbital times, followed by the formation of a thick hot accretion disk around the more-massive companion. The further evolution hinges crucially on the effective accretion rate of the disk: In case \dot{M} is larger than a few times $10^{-6} M_{\odot} \text{ year}^{-1}$, the most likely outcome is off-center carbon ignition leading to an inward propagating flame that converts the star into O + Ne + Mg (Nomoto & Iben 1985, Saio & Nomoto 1985, Kawai et al 1987, Timmes et al 1994, Saio & Nomoto 1998). This configuration, in turn, is gravitationally unstable owing to electron capture onto ^{24}Mg and will undergo accretion-induced collapse to form a neutron star (Saio & Nomoto 1985, Mochkovitch & Livio 1990, Nomoto & Kondo 1991). A recent reexamination of Coulomb corrections to the equation of state of material in nuclear statistical equilibrium indicates that accretion-induced collapse in merged white dwarf systems is even more likely than previously anticipated (Bravo & Garcia-Senz 1999).

Dimensional analysis of the expected turbulent viscosity due to magneto-hydrodynamical (MHD) instabilities (Balbus et al 1996) suggests that it is very difficult to avoid such high accretion rates (Mochkovitch & Livio 1990, Livio 1999). Even under the unphysical assumption that angular momentum transport is dominated entirely by microscopic electron-gas viscosity, the expected life time of $\sim 10^9$ years (Mochkovitch & Livio 1990, Mochkovitch et al 1997) and high UV luminosity of these accretion systems would predict the existence of $\sim 10^7$ such objects in the Galaxy, none of which have been observed (Livio 1999).

A possible solution to the collapse problem is to ignite carbon burning as a detonation rather than a flame immediately during the merger event, either in the core of the more massive star (Shigeyama et al 1992) or at the contact surface (D Arnett & PA Pinto, private communication). This alternative clearly warrants further study.

To summarize, the merging white dwarf scenario must overcome the crucial problem of avoiding accretion-induced collapse before it can be seriously considered as a SN Ia candidate. Its key strengths are a plausible explanation for the progenitor history, yielding reasonable predictions for SN Ia rates, the straightforward explanation of the absence of H and He in SN Ia spectra, and the existence of a simple parameter for the explosion strength family (i.e. the mass of the merged system).

6. SUMMARY

In this review we have outlined our current understanding of type Ia supernovae, summarizing briefly the observational constraints, but putting more weight on models of the explosion. From the tremendous amount of work carried out over the past couple of years, it has become obvious that the physics of SNe Ia is

complex, ranging from the possibility of different progenitors to the complexity of the physics leading to the explosion and the complicated processes that couple the interior physics to observable quantities. None of these problems is fully understood yet, but what one is tempted to state is that, from a theorist's point of view, it appears to be a miracle that all the complexity seems to average out in a mysterious way to make the class so homogeneous. In contrast, as it stands, a safe prediction from theory seems to be that SNe Ia should get more diverse with increasing observed sample sizes. If, however, homogeneity would continue to hold, this would certainly add support to the Chandrasekhar-mass single-degenerate scenario. On the other hand, even an increasing diversity would not rule out Chandrasekhar-mass single-degenerate progenitors for most of them. In contrast, there are ways to explain how the diversity is absorbed in a one-parameter family of transformations, such as the Phillips relation or modifications of it. For example, we have argued that the size of the convective core of the white dwarf prior to the explosion might provide a physical reason for such a relation.

As far as the explosion /combustion physics and the numerical simulations are concerned, significant recent progress has made the models more realistic (and reliable). Thanks to ever increasing computer resources, 3D simulations that treat the full star with good spatial resolution and realistic input physics have become feasible. Already the results of 2D simulations indicate that pure deflagrations waves in Chandrasekhar-mass C + O white dwarfs can lead to explosions, and one can expect that going to three dimensions, because of the increasing surface area of the nuclear flames, should add to the explosion energy. If confirmed, this would eliminate pulsational detonations from the list of potential models. On the side of the combustion physics, the burning in the distributed regime at low densities needs to be explored further, but it is not clear anymore whether a transition from a deflagration to a detonation in that regime is needed for successful models. In fact, according to recent studies, such a transition appears to be unlikely.

Finally, sub-Chandrasekhar-mass models seem to face problems, both from the observations and from theory, leaving us with the conclusion that we seem to be lucky and Nature was kind to us and singled out from all possibilities the simplest solution, namely a Chandrasekhar-mass C + O white dwarf and a nuclear deflagration wave, to make a type Ia supernova explosion.

Visit the Annual Reviews home page at www.AnnualReviews.org

LITERATURE CITED

- Aldering G, Knop R, Nugent P. 2000. *Astron J.*
In press
- Arnett WD. 1969. *Astrophys. Space Sci.* 5:180–212
- Arnett WD. 1971. *Ap. J.* 169:113
- Arnett WD. 1996. *Supernovae and Nucleosynthesis*. Princeton: Princeton Univ. Press
- Arnett WD. 1997. In Ruiz-Lapuente, Canal, & Isern 1997, pp. 405–40
- Arnett WD, Livne E. 1994a. *Ap. J.* 427:315–29
- Arnett WD, Livne E. 1994b. *Ap. J.* 427:330–41

- Arnett WD, Truran JW, Woosley SE. 1971. *Ap. J.* 165:87
- Axelrod TS. 1980. *Late time optical spectra from the Ni-56 model for Type 1 supernovae*. Ph.D. thesis, Univ. Calif., Santa Cruz
- Baade W, Zwicky F. 1934. *Phys. Rev.* 46:76
- Balbus SA, Hawley JF, Stone JM. 1996. *Ap. J.* 467:76
- Barkat Z, Wheeler JC. 1990. *Ap. J.* 355:602–16
- Baron E, Hauschildt PH, Mezzacappa A. 1997. In Ruiz-Lapuente, Canal, & Isern 1997, pp. 627–46
- Bartunov OS, Tsvetkov DY, Filimonova IV. 1994. *PASP* 106:1276–84
- Beer A. 1974. *Vistas in Astronomy*, vol. 16. Oxford: Pergamon
- Benson PJ, Little-Marenin IR, Herbst W, Salzer JJ, Vinton G, et al. 1993. *Am. Astron. Soc. Meet.*, vol. 182, p. 2916. Washington DC: Am. Astron. Soc.
- Benz W. 1997. In Ruiz-Lapuente, Canal, & Isern 1997, pp. 457–74
- Benz W, Cameron AGW, Press WH, Bowers RL. 1990. *Ap. J.* 348:647–67
- Blanco VM. 1987. In *ESO Workshop SN 1987 A*, ed. IF Danziger, pp. 27–32. Garching, Ger: Europ. South. Obs.
- Blinnikov SI. 1996. In *Proc. 8th Workshop on Nuclear Astrophysics*, eds. W Hillebrandt, E Müller, pp. 25–9. Garching, Ge: Max-Planck-Inst. Astrophys.
- Blinnikov SI. 1997. In Ruiz-Lapuente, Canal, & Isern 1997, pp. 589–95
- Blinnikov SI, Khokhlov AM. 1986. *Sov. Astron. Lett.* 12:131
- Blinnikov SI, Khokhlov AM. 1987. *Sov. Astron.* 13:364
- Blinnikov SI, Nadyoshin DK. 1991. The shock breakout in SN1987a modelled with the time-dependent radiative transfer. *Tech. Rep. N92-1293303-90*, Sternberg Astron. Inst., Moscow
- Blinnikov SI, Sasorov PV. 1996. *Phys. Rev. E* 53:4827
- Boffi FR, Branch D. 1995. *PASP* 107:347
- Boisseau JR, Wheeler JC, Oran ES, Khokhlov AM. 1996. *Ap. J. Lett.* 471:L99
- Bragaglia A. 1997. In Ruiz-Lapuente, Canal, & Isern 1997, pp. 231–37
- Branch D. 1981. *Ap. J.* 248:1076–80
- Branch D. 1998. *Annu. Rev. Astron. Astrophys.* 36:17–56
- Branch D, Fisher A, Nugent P. 1993. *Astron. J.* 106:2383–91
- Branch D, Romanishin W, Baron E. 1996. *Ap. J.* 465:73
- Branch D, Tammann GA. 1992. *Annu. Rev. Astron. Astrophys.* 30:359–89
- Branch D, Venkatakrishna KL. 1986. *Ap. J. Lett.* 306:L21–3
- Bravo E, Garcia-Senz D. 1995. *Ap. J. Lett.* 450:L17
- Bravo E, Garcia-Senz D. 1997. *Proc. IAU Symp.* 187, p. E3
- Bravo E, Garcia-Senz D. 1999. *MNRAS* 307:984–92
- Bruenn SW. 1973. *Ap. J. Lett.* 183:L125
- Buchler JR, Colgate SA, Mazurek TJ. 1980. *J. Phys.* 41:2–159
- Buchler JR, Mazurek TJ. 1975. *Mem. Soc. R. Sci. Liege* 8:435–45
- Burrows A, Shankar A, van Riper KA. 1991. *Ap. J. Lett.* 379:L7–11
- Burrows A, The LS. 1990. *Ap. J.* 360:626–38
- Bychkov VV, Liberman MA. 1995a. *Astron. Astrophys.* 302:727
- Bychkov VV, Liberman MA. 1995b. *Ap. J.* 451:711
- Cappellaro E, Turatto M, Tsvetkov D, Bartunov O, Pollas C, et al. 1997. *Astron. Astrophys.* 322:431–41
- Cassisi S, Castellani V, Tornambe A. 1996. *Ap. J.* 459:298
- Cassisi S, Iben I. J, Tornambe A. 1998. *Ap. J.* 496:376
- Chandrasekhar S. 1961. *Hydrodynamic and Hydromagnetic Stability*. Oxford: Oxford Univ. Press
- Clavin P. 1994. *Annu. Rev. Fluid Mech.* 26:321
- Colgate SA, McKee C. 1969. *Ap. J.* 157:623
- Contardo G. 1999. In *Future Directions in Supernova Research: Progenitors to Remnants*. In press
- Contardo G, Leibundgut B. 1998. In *Proc. 9th*

- Workshop Nucl. Astrophys.*, eds. W Hillebrandt, E Müller, p. 128. Garching, Ger: Max-Planck-Inst. Astrophys.
- Courant R, Friedrichs KO. 1948. *Supersonic Flow and Shock Waves*. New York: Springer
- Cox JP, Giuli RT. 1968. *Principles of Stellar Structure*, vol. II, pp. 183–261. New York: Gordon & Breach
- Cumming RJ, Lundqvist P, Smith LJ, Pettini M, King DL. 1996. *MNRAS* 283:1355–60
- Damköhler G. 1940. *Z. Elektrochem.* 46:601
- Darrieus G. 1944. *La Tech. Mod.* Unpublished
- Di Stefano R, Rappaport S. 1994. *Ap. J.* 437: 733–41
- Eastman RG. 1997. In Ruiz-Lapuente, Canal, & Isern 1997, pp. 571–88
- Eastman RG, Pinto PA. 1993. *Ap. J.* 412:731–51
- Eck CR, Cowan JJ, Roberts DA, Boffi FR, Branch D. 1995. *Ap. J. Lett.* 451: L53
- Elias JH, Matthews K, Neugebauer G, Persson SE. 1985. *Ap. J.* 296:379–89
- Fermi E. 1951. In *Collected Works of Enrico Fermi*, ed. E Segre, pp. 816–21. Chicago: Univ. Chicago Press
- Filippenko AV. 1988. *Astron. J.* 96:1941–8
- Filippenko AV. 1997a. *Annu. Rev. Astron. Astrophys.* 35:309–55
- Filippenko AV. 1997b. In Ruiz-Lapuente, Canal, & Isern 1997, pp. 1–32
- Filippenko AV, Richmond MW, Branch D, Gaskell M, Herbst W, et al. 1992a. *Astron. J.* 104:1543–56
- Filippenko AV, Richmond MW, Matheson T, Shields JC, Burbidge EM, et al. 1992b. *Ap. J. Lett.* 384:L15–8
- Filippenko AV, Riess AG. 2000. See Niemeyer & Truran 2000
- Fisher A, Branch D, Hatano K, Baron E. 1999. *MNRAS* 304:67–74
- Fryer C, Benz W, Herant M, Colgate SA. 1999. *Ap. J.* 516:892–9
- Fu A. 1987. *Ap. J.* 323:227–42
- Gamezo VN, Wheeler JC, Khokhlov AM, Oran ES. 1999. *Ap. J.* 512:827–42
- Garcia-Senz D, Bravo E, Serichol N. 1998. *Ap. J. suppl.* 115:119
- Garcia-Senz D, Bravo E, Woosley SE. 1999. *Astron. Astrophys.* 349:177–88
- Garcia-Senz D, Woosley SE. 1995. *Ap. J.* 454:895
- Garnavich PM, Jha S, Challis P, Clocchiatti A, Diercks A, et al. 1998. *Ap. J.* 509:74–9
- Gehrz RD, Truran JW, Williams RE. 1993. In *Protostars and Planets*, ed. E Levy, pp. 75–95. Tucson: Univ. Arizona Press
- Gilmozzi R. 1987. In *ESO Workshop SN 1987 A*, ed. IF Danziger, pp. 19–24. Garching, Ger: Europ. South. Obs.
- Gilmozzi R, Cassatella A, Clavel J, Gonzalez R, Fransson C. 1987. *Nature* 328:318–20
- Goobar A, Perlmutter S. 1995. *Ap. J.* 450:14
- Greiner J, Hasinger G, Kahabka P. 1991. *Astron. Astrophys.* 246:L17–20
- Hachisu I, Kato M, Nomoto K. 1996. *Ap. J. Lett.* 470:L97
- Hachisu I, Kato M, Nomoto Ki. 1999a. *Ap. J.* 522:487–503
- Hachisu I, Kato M, Nomoto Ki, Umeda H. 1999b. *Ap. J.* 519:314–23
- Hamuy M, Phillips MM, Maza J, Suntzeff NB, Della Valle M, et al. 1994. *Astron. J.* 108:2226–32
- Hamuy M, Phillips M, Suntzeff NB, Schommer RA, Maza J, et al. 1996a. *Astron. J.* 112:2391
- Hamuy M, Phillips MM, Maza J, Suntzeff NB, Schommer RA, et al. 1995. *Astron. J.* 109:1–13
- Hamuy M, Phillips MM, Suntzeff NB, Schommer RA, Maza J, et al. 1996b. *Astron. J.* 112:2398
- Hamuy M, Phillips MM, Suntzeff NB, Schommer RA, Maza J, et al. 1996c. *Astron. J.* 112:2438
- Hansen CJ, Kawaler SD. 1994. *Stellar Interiors*, p. 247 New York: Springer
- Hansen CJ, Wheeler JC. 1969. *Astrophys. Space Sci.* 3:464
- Harkness RP. 1991. In *Supernova 1987A and Other Supernovae, Conf. Proc. 37*, eds. IJ Danziger, K Kjär, pp. 447–56. Garching, Ger: Europ. South. Obs.

- Hatano K, Branch D, Baron E. 1998. In *Am. Astron. Soc. Meet.*, vol. 193, p. 4703
- Hillebrandt W, Hoeflich P, Weiss A, Truran JW. 1987. *Nature* 327:597–600
- Hoeflich P. 1995. *Ap. J.* 443:89–108
- Hoeflich P, Khokhlov A. 1996. *Ap. J.* 457:500
- Hoeflich P, Khokhlov A, Müller E. 1992. *Astron. Astrophys.* 259:549–66
- Hoeflich P, Khokhlov A, Wheeler JC, Nomoto K, Thielemann FK. 1997. In Ruiz-Lapuente, Canal, & Isern 1997, pp. 659–79
- Hoeflich P, Khokhlov AM, Wheeler JC. 1995. *Ap. J.* 444:831–47
- Hoeflich P, Wheeler JC, Khokhlov A. 1998a. *Ap. J.* 492:228
- Hoeflich P, Wheeler JC, Thielemann FK. 1998b. *Ap. J.* 495:617
- Homeier U, Koester D, Hagen HJ, Jordan S, Heber U, et al. 1998. *Astron. Astrophys.* 338:563–75
- Hoyle F, Fowler WA. 1960. *Ap. J.* 132:565
- Iben I. J. 1978. *Ap. J.* 219:213–25
- Iben I. J. 1982. *Ap. J.* 253:248–59
- Iben I. J, Tutukov AV. 1984. *Ap. J. suppl.* 54:335–72
- Imshennik VS, Kal'Yanova NL, Koldoba AV, Chechetkin VM. 1999. *Astron. Lett.* 25:206–14
- Imshennik VS, Khokhlov AM. 1984. *Sov. Astron. Lett.* 10:262
- Ivanova LN, Imshennik VS, Chechetkin VM. 1974. *Astrophys. Space Sci.* 31:497–514
- Ivanova LN, Imshennik VS, Chechetkin VM. 1982. *Pisma Astron. Zhurnal* 8:17–25
- Iwamoto K, Brachwitz F, Nomoto KI, Kishimoto N, Umeda H, et al. 1999. *Ap. J. suppl.* 125:439–62
- Jeffery DJ, Leibundgut B, Kirshner RP, Benetti S, Branch D, et al. 1992. *Ap. J.* 397:304–28
- Kahabka P, Van Den Heuvel EPJ. 1997. *Annu. Rev. Astron. Astrophys.* 35:69–100
- Karp AH, Lasher G, Chan KL, Salpeter EE. 1977. *Ap. J.* 214:161–78
- Kato M, Hachisu I. 1999. *Ap. J. Lett.* 513:L41–4
- Kawai Y, Saio H, Nomoto KI. 1987. *Ap. J.* 315:229–33
- Kercek A, Hillebrandt W, Truran JW. 1999. *Astron. Astrophys.* 345:831–40
- Kerstein AR. 1996. *Combust. Sci. Technol.* 118:189
- Khokhlov AM. 1988. *Astrophys. Space Sci.* 149:91–106
- Khokhlov AM. 1989. *MNRAS* 239:785–808
- Khokhlov AM. 1991a. *Astron. Astrophys.* 245:114–28
- Khokhlov AM. 1991b. *Astron. Astrophys.* 245:L25–28
- Khokhlov AM. 1993a. *Ap. J. Lett.* 419:L77
- Khokhlov AM. 1993b. *Ap. J.* 419:200
- Khokhlov AM. 1994. *Ap. J. Lett.* 424:L115–17
- Khokhlov AM. 1995. *Ap. J.* 449:695
- Khokhlov AM, Müller E, Hoeflich P. 1993. *Astron. Astrophys.* 270:223–48
- Khokhlov AM, Oran ES, Wheeler JC. 1997. *Ap. J.* 478:678
- King AR, Van Teeseling A. 1998. *Astron. Astrophys.* 338:965–70
- Kippenhahn R, Weigert A. 1989. *Stellar Structure and Evolution*. Berlin: Springer
- Kobayashi C, Tsujimoto T, Nomoto KI, Hachisu I, Kato M. 1998. *Ap. J. Lett.* 503:L155
- Koen C, Orosz JA, Wade RA. 1998. *MNRAS* 300:695–704
- Kolmogorov AN. 1941. *Dokl. Akad. Nauk SSSR* 30:299
- Kriminski SA, Bychkov VV, Liberman M. 1998. *New Astron.* 3:363–77
- Kuchner MJ, Kirshner RP, Pinto PA, Leibundgut B. 1994. *Ap. J. Lett.* 426:L89
- Kunasz PB. 1984. *Ap. J.* 276:677–90
- Landau LD. 1944. *Acta Physicochim. URSS* 19:77
- Landau LD, Lifshitz EM. 1995. *Fluid Mechanics*. London: Pergamon
- Layzer D. 1955. *Ap. J.* 122:1
- Lee JHS, Knystautas R, Yoshikawa N. 1978. *Acta Astronaut.* 5:971
- Leibundgut B, Kirshner RP, Phillips MM, Wells LA, Suntzeff N, et al. 1993. *Astron. J.* 105:301–13
- Leising MD, Johnson WN, Kurfess JD,

- Clayton DD, Grabelsky DA, et al. 1995. *Ap. J.* 450:805
- Lentz EJ, Baron E, Branch D, Hauschildt PH, Nugent PE. 1999. In *Am. Astron. Soc. Meet.*, vol.194, p. 8606
- Lentz EJ, Baron E, Branch D, Hauschildt PH, Nugent PE. 2000. *Ap. J.* 530:966–76
- Lewis B, von Elbe G. 1961. *Combustion, Flames, and Explosions of Gases*. New York: Academic
- Li WD, Filippenko AV, Riess AG, Hu JY, Qiu YL. 2000. In *Proc. 10th Ann. Oct. Astrophys. Conf. Cosmic Explosions*. Univ. Maryland. In press
- Livio M. 1996. In *Supersoft X-ray Sources, Proc. Int. Workshop*, ed. J Greiner, vol. 472, pp. 183–91. Garching, Ger: Max-Planck-Inst. Extraterr. Phys.
- Livio M. 2000. In Niemeyer & Truran 2000
- Livio M, Branch D, Yungelson LB, Boffi F, Baron E. 1996. In *IAU Colloq. 158: Cataclysmic Variables and Related Objects*, pp. 407–15
- Livne E. 1990. *Ap. J. Lett.* 354:L53–5
- Livne E. 1993. *Ap. J. Lett.* 406:L17–20
- Livne E. 1997. In Ruiz-Lapuente, Canal, & Isern 1997, pp. 425–40
- Livne E, Arnett D. 1995. *Ap. J.* 452:62
- Livne E, Glasner AS. 1991. *Ap. J.* 370:272–81
- Lucy LB. 1999. *Astron. Astrophys.* 345:211–20
- Lundmark K. 1920. *Svenska Vetenskapsakad. Handl.* 60:8
- Lundmark K. 1921. *Publ. Astron. Soc. Pac.* 33:234
- Lundqvist P, Cumming RJ. 1997. In *Advances in Stellar Evolution*, pp. 293–6. Cambridge, UK: Cambridge Univ. Press
- Mair G, Hillebrandt W, Hoefflich P, Dorfi A. 1992. *Astron. Astrophys.* 266:266–82
- Mazzali PA, Chugai N, Turatto M, Lucy LB, Danziger IJ, et al. 1997a. *MNRAS* 284:151–71
- Mazzali PA, Danziger IJ, Turatto M. 1995. *Astron. Astrophys.* 297:509
- Mazzali PA, Lucy LB. 1993. *Astron. Astrophys.* 279:447–56
- Mazzali PA, Turatto M, Cappellaro E, Della Valle M, Benetti S, et al. 1997b. In Ruiz-Lapuente, Canal, & Isern 1997, pp. 647–58
- Meikle WPS, Bowers EJC, Geballe TR, Walton NA, Lewis JR, et al. 1997. In Ruiz-Lapuente, Canal, & Isern 1997, pp. 53–64
- Meikle WPS, Cumming RJ, Geballe TR, Lewis JR, Walton NA, et al. 1996. *MNRAS* 281:263–80
- Mihalas D, Weibel Mihalas B. 1984. *Foundations of Radiation Hydrodynamics*. New York: Oxford Univ. Press
- Minkowski R. 1940. *Publ. Astron. Soc. Pac.* 52:206
- Mochkovitch R. 1996. *Astron. Astrophys.* 311:152–4
- Mochkovitch R, Guerrero J, Segretain L. 1997. In Ruiz-Lapuente, Canal, & Isern 1997, pp. 187–204
- Mochkovitch R, Livio M. 1990. *Astron. Astrophys.* 236:378–84
- Morris DJ, Bennett K, Bloemen H, Diehl R, Hermesen W, et al. 1997. In *AIP Conf. Proc. 410. Proc. 4th Compton Symp.*, p. 1084
- Müller E. 1998. In *Computational Methods for Astrophysical Fluid Flow*, eds. O Steiner, A Gautschi, pp. 343–494. Berlin, New York: Springer
- Müller E, Arnett WD. 1982. *Ap. J. Lett.* 261:L109–15
- Müller E, Arnett WD. 1986. *Ap. J.* 307:619–43
- Müller E, Hoefflich P, Khokhlov A. 1991. *Astron. Astrophys.* 249:L1–4
- Munari U, Renzini A. 1992. *Ap. J. Lett.* 397:L87–90
- Nandkumar R, Pethick CJ. 1984. *MNRAS* 209:511–24
- Niemeyer JC. 1999. *Ap. J. Lett.* 523:L57–60
- Niemeyer JC, Bushe WK, Ruetsch GR. 1999. *Ap. J.* 524:290
- Niemeyer JC, Hillebrandt W. 1995a. *Ap. J.* 452:779
- Niemeyer JC, Hillebrandt W. 1995b. *Ap. J.* 452:769
- Niemeyer JC, Hillebrandt W. 1997. In Ruiz-Lapuente, Canal, & Isern 1997, pp. 441–56

- Niemeyer JC, Hillebrandt W, Woosley SE. 1996. *Ap. J.* 471:903
- Niemeyer JC, Kerstein AR. 1997. *New Astron.* 2:239–44
- Niemeyer JC, Truran JW, eds. 2000. *Type Ia Supernovae: Theory and Cosmology*, Cambridge: Cambridge Univ. Press
- Niemeyer JC, Woosley SE. 1997. *Ap. J.* 475:740
- Nomoto K. 1980. *Space Sci. Rev.* 27:563–70
- Nomoto K. 1982a. *Ap. J.* 257:780–92
- Nomoto K. 1982b. *Ap. J.* 253:798–810
- Nomoto K, Iben I. J. 1985. *Ap. J.* 297:531–7
- Nomoto K, Iwamoto K, Thielemann F, Brachwitz F, et al. 1997. In Ruiz-Lapuente, Canal, & Isern 1997, pp. 349–78
- Nomoto K, Iwamoto K, Yamaoka H, Hashimoto M. 1995. In *ASP Conf. Ser. 72: Millisecond Pulsars. A Decade of Surprise*, p. 164
- Nomoto K, Nariai K, Sugimoto D. 1979. *Publ. Astron. Soc. Jpn.* 31:287–98
- Nomoto K, Sugimoto D. 1977. *Publ. Astron. Soc. Jpn.* 29:765–80
- Nomoto K, Sugimoto D, Neo S. 1976. *Astrophys. Space Sci.* 39:L37–42
- Nomoto K, Suzuki T, Shigeyama T, Kumagai S, Yamaoka H, et al. 1993. *Nature* 364:507–9
- Nomoto K, Thielemann FK, Yokoi K. 1984. *Ap. J.* 286:644–58
- Nomoto K, Yamaoka H, Pols OR, Van den Heuvel EPJ, Iwamoto K, et al. 1994a. *Nature* 371:227
- Nomoto K, Yamaoka H, Shigeyama T, Iwamoto K. 1996. In *Supernovae and Supernova Remnants. Proc. IAU Colloq. 145. Xian, China*, eds. R McCray, Z Wang, pp. 49–68. Cambridge: Cambridge Univ. Press
- Nomoto K, Yamaoka H, Shigeyama T, Kumagai S, Tsujimoto T. 1994b. In *Supernovae, Les Houches Session LIV*, eds. J Audouze, S Bludman, R Mochovitch, J Zinn-Justin, pp. 199–249. Amsterdam: Elsevier
- Nomoto KI, Kondo Y. 1991. *Ap. J. Lett.* 367:L19–22
- Nugent P, Baron E, Branch D, Fisher A, Hauschildt PH. 1997. *Ap. J.* 485:812
- Nugent P, Baron E, Hauschildt PH, Branch D. 1995. *Ap. J. Lett.* 441:L33–6
- Paczynski B. 1972. *Ap. J.* 11:L53
- Paczynski B. 1973. *Astron. Astrophys.* 26:291
- Paczynski B. 1985. In *Cataclysmic variables and low-mass X-ray binaries. Proc. 7th North Am. Workshop*, pp. 1–12. Dordrecht: Reidel
- Pakull MW, Moch C, Bianchi L, Thomas HC, Guibert J, et al. 1993. *Astron. Astrophys.* 278:L39–42
- Patat F, Benetti S, Cappellaro E, Danziger IJ, Della Valle M, et al. 1996. *MNRAS* 278:111–24
- Pauldrach AWA, Duschinger M, Mazzali PA, Puls J, Lennon M, et al. 1996. *Astron. Astrophys.* 312:525–38
- Perlmutter S, Aldering G, Goldhaber G, Knop RA, Nugent P, et al. 1999. *Ap. J.* 517:565–86
- Perlmutter S, Gabi S, Goldhaber G, Goobar A, Groom DE, et al. 1997. *Ap. J.* 483:565
- Peters N. 1988. In *Symp. Int. Combust., 21st*, p. 1232. Pittsburgh: Combust. Inst.
- Phillips MM. 1993. *Ap. J. Lett.* 413:L105–8
- Phillips MM, Wells LA, Suntzeff NB, Hamuy M, Leibundgut B, et al. 1992. *Astron. J.* 103:1632–37
- Pinto PA. 1997. In Ruiz-Lapuente, Canal, & Isern 1997, pp. 607–27
- Podsiadlowski P. 1993. *Space Sci. Rev.* 66:439
- Pope SB. 1987. *Annu. Rev. Fluid Mech.* 19:237–70
- Popper DM. 1937. *Publ. Astron. Soc. Pac.* 49:283
- Pskovskii IP. 1977. *Sov. Astron.* 21:675–82
- Rasio FA, Shapiro SL. 1995. *Ap. J.* 438:887–903
- Rayleigh LK. 1883. *Proc. London Math. Soc.* 14:170
- Read KI. 1984. *Physica D* 12:45
- Reinecke M, Hillebrandt W, Niemeyer JC. 1999a. *Astron. Astrophys.* 347:739–47
- Reinecke M, Hillebrandt W, Niemeyer JC, Klein R, Gröbl A. 1999b. *Astron. Astrophys.* 347:724–33

- Renzini A. 1996. In *Supernovae and Supernova Remnants. Proc. IAU Colloq. 145. Xian, China*, eds. R McCray, Z Wang, p. 77. Cambridge: Cambridge Univ. Press
- Riess AG, Filippenko AV, Challis P, Clocchiatti A, Diercks A, et al. 1998. *Astron. J.* 116:1009–38
- Riess AG, Filippenko AV, Li W, Schmidt BP. 1999a. *Astron. J.* 118:2668–74
- Riess AG, Filippenko AV, Li W, Treffers RR, Schmidt BP, et al. 1999b. *Astron. J.* 118:2675–88
- Riess AG, Press WH, Kirshner RP. 1996. *Ap. J.* 473:88
- Ruiz-Lapuente P. 1997. In Ruiz-Lapuente, Canal, & Isern 1997, pp. 681–704
- Ruiz-Lapuente P, Burkert A, Canal R. 1995. *Ap. J. Lett.* 447:L69
- Ruiz-Lapuente P, Canal R. 1998. *Ap. J. Lett.* 497:L57
- Ruiz-Lapuente P, Canal R, Isern J, eds. 1997. *Thermonuclear Supernovae*, Dordrecht. Kluwer
- Ruiz-Lapuente P, Cappellaro E, Turatto M, Gouiffes C, Danziger IJ, et al. 1992. *Ap. J. Lett.* 387:L33–6
- Ruiz-Lapuente P, Jeffery DJ, Challis PM, Filippenko AV, Kirshner RP, et al. 1993a. *Nature* 365:728
- Ruiz-Lapuente P, Lichi GG, Lehoucq R, Canal R, Casse M. 1993b. *Ap. J.* 417:547
- Saffer RA, Livio M, Yungelson LR. 1998. *Ap. J.* 502:394
- Saio H, Nomoto K. 1985. *Astron. Astrophys.* 150:L21–3
- Saio H, Nomoto KI. 1998. *Ap. J.* 500:388–97
- Schmidt BP, Kirshner RP, Eastman RG, Grashuis R, Dell’Antonio I, et al. 1993. *Nature* 364:600–2
- Schmidt BP, Suntzeff NB, Phillips MM, Schommer RA, Clocchiatti A, et al. 1998. *Ap. J.* 507:46–63
- Schoenfelder V, Bennett K, Bloemen H, Diehl R, Hermesen W, et al. 1996. *Astron. Astrophys. Suppl.* 120:C13
- Sharp DH. 1984. *Physica D* 12:3
- Shigeyama T, Kumagai S, Yamaoka H, Nomoto K, Thielemann FK. 1993. *Astron. Astrophys. Suppl.* 97:223–4
- Shigeyama T, Nomoto Ki, Yamaoka H, Thielemann FK. 1992. *Ap. J. Lett.* 386:L13–6
- Sorokina EI, Blinnikov SI, Bartunov OS. 1999. In *Proc. Astron. at the Eve of the New Century*
- Southwell KA, Livio M, Charles PA, O’Donoghue D, Sutherland WJ. 1996. *Ap. J.* 470:1065
- Sparks WM, Starrfield S, Truran JW. 1976. *Ap. J.* 208:819–25
- Spyromilio J, Meikle WPS, Allen DA, Graham JR. 1992. *MNRAS* 258:53P–56P
- Spyromilio J, Pinto PA, Eastman RG. 1994. *MNRAS* 266:L17
- Starrfield S, Truran JW, Sparks WM. 1978. *Ap. J.* 226:186–202
- Starrfield S, Truran JW, Sparks WM, Kutter GS. 1972. *Ap. J.* 176:169
- Stein J, Barkat Z, Wheeler JC. 1999. *Ap. J.* 523:381–5
- Stone JM, Mihalas D, Norman ML. 1992. *Ap. J. suppl.* 80:819–45
- Suntzeff NB. 1996. In *Supernovae and Supernova Remnants. Proc. IAU Colloq. 145. Xian, China*, eds. R McCray, Z Wang, p. 41. Cambridge: Cambridge Univ. Press
- Sutherland PG, Wheeler JC. 1984. *Ap. J.* 280:282–97
- Thielemann FK, Nomoto K, Yokoi K. 1986. *Astron. Astrophys.* 158:17–33
- Timmes FX. 1999. *Ap. J. Suppl.* 124:241
- Timmes FX, Woosley SE. 1992. *Ap. J.* 396:649–67
- Timmes FX, Woosley SE. 1997. *Ap. J.* 489:160
- Timmes FX, Woosley SE, Taam RE. 1994. *Ap. J.* 420:348–63
- Tripp R. 1998. *Astron. Astrophys.* 331:815–20
- Truemper J, Hasinger G, Aschenbach B, Braeuninger H, Briel UG. 1991. *Nature* 349:579–83
- Truran JW. 1982. In *Essays in Nuclear Astrophysics*, eds. C Barnes, DD Clayton, DN Schramm, WA Fowler, p. 467. Cambridge: Cambridge Univ. Press
- Truran JW, Arnett D, Cameron AGW. 1967. *Canad. J. Physics* 45:2315–32

- Turatto M, Benetti S, Cappellaro E, Danziger IJ, Della Valle M, et al. 1996. *MNRAS* 283:1–17
- Tutukov A, Yungelson L. 1996. *MNRAS* 280:1035–45
- Umeda H, Nomoto K, Kobayashi C, Hachisu I, Kato M. 1999. *Ap. J. Lett.* 522:L43–7
- Van den Heuvel EPJ, Bhattacharya D, Nomoto K, Rappaport SA. 1992. *Astron. Astrophys.* 262:97–105
- Vaughan TE, Branch D, Miller DL, Perlmutter S. 1995. *Ap. J.* 439:558–64
- Wang L, Hoefflich P, Wheeler JC. 1997. *Ap. J. Lett.* 483:L29
- Watanabe K, Hartmann DH, Leising MD, The LS. 1999. *Ap. J.* 516:285–96
- Weaver TA, Woosley SE. 1980. In *AIP Conf. Proc.* 63. *Supernovae Spectra*. La Jolla, CA, p. 15
- Webbink RF. 1984. *Ap. J.* 277:355–60
- Wellstein S, Langer N. 1999. *Astron. Astrophys.* 350:148–62
- Wheeler JC, Harkness RP. 1990. *Rep. Prog. Phys.* 53:1467–557
- Wheeler JC, Hoefflich P, Harkness RP, Spyromilio J. 1998. *Ap. J.* 496:908
- Whelan J, Iben I. J. 1973. *Ap. J.* 186:1007–14
- Wiggins DJR, Falle SAEG. 1997. *MNRAS* 287:575–82
- Wiggins DJR, Sharpe GJ, Falle SAEG. 1998. *MNRAS* 301:405–13
- Williams FA. 1985. *Combustion Theory*. Menlo Park, CA: Benjamin/Cummings
- Wilson OC. 1939. *Ap. J.* 90:634
- Woosley SE. 1990. In *Supernovae*, ed. AG Petschek, pp. 182–210. Berlin: Springer-Verlag
- Woosley SE. 1997a. *Ap. J.* 476:801
- Woosley SE. 1997b. In Ruiz-Lapuente, Canal, & Isern 1997, pp. 313–37
- Woosley SE, Axelrod TS, Weaver TA. 1984. In *Stellar Nucleosynthesis*, eds. C Chiosi, A Renzini, p. 263. Dordrecht: Kluwer
- Woosley SE, Taam RE, Weaver TA. 1986. *Ap. J.* 301:601–23
- Woosley SE, Weaver TA. 1986a. *Annu. Rev. Astron. Astrophys.* 24:205–53
- Woosley SE, Weaver TA. 1986b. In *Radiation Hydrodynamics in Stars and Compact Objects*, *Lect. Notes Phys.*, eds. D Mihalas, KHA Winkler, vol. 255, p. 91. Berlin: Springer-Verlag
- Woosley SE, Weaver TA. 1994a. In *Supernovae, Les Houches Session LIV*, eds. J Audouze, S Bludman, R Mochovitich, J Zinn-Justin, p. 63. Amsterdam: Elsevier
- Woosley SE, Weaver TA. 1994b. *Ap. J.* 423:371–79
- Woosley SE, Weaver TA, Taam RE. 1980. In *Texas Workshop Type I Supernovae*, ed. J Wheeler, pp. 96–112. Austin, TX: Univ. Texas
- Yin WW, Miller GS. 1995. *Ap. J.* 449:826
- Youngs DL. 1984. *Physica D* 12:32
- Yungelson L, Livio M. 1998. *Ap. J.* 497: 168
- Yungelson L, Livio M, Truran JW, Tutukov A, Fedorova A. 1996. *Ap. J.* 466:890
- Zeldovich YB. 1966. *J. Appl. Mech. and Tech. Phys.* 7:68
- Zeldovich YB, Barenblatt GI, Librovich VB, Makhviladze GM. 1985. *The Mathematical Theory of Combustion and Explosions*. New York: Plenum
- Zeldovich YB, Librovich VB, Makhviladze GM, Sivashinsky GL. 1970. *Astronaut. Acta* 15:313
- Zwicky F. 1938a. *Phys. Rev.* 55:726
- Zwicky F. 1938b. *Ap. J.* 88:522
- Zwicky F. 1965. In *Stellar Structure*, eds. LH Aller, DB McLaughlin, pp. 367–424. Chicago: Univ. of Chicago Press

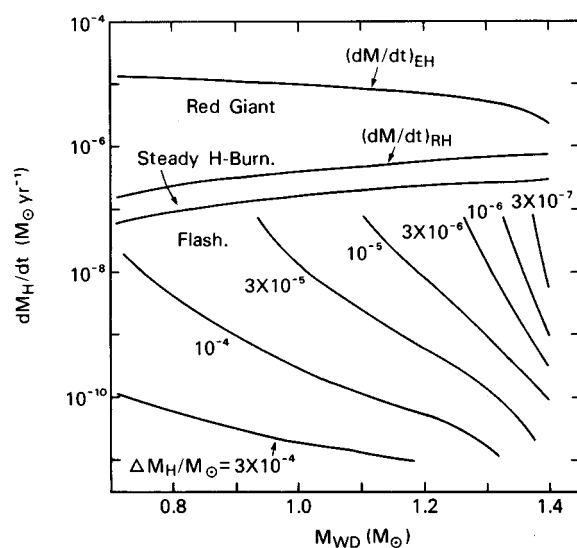


Figure 2 The likely outcome of hydrogen accretion onto white dwarfs of different masses is shown. From Kahabka and Van Den Heuvel (1997).

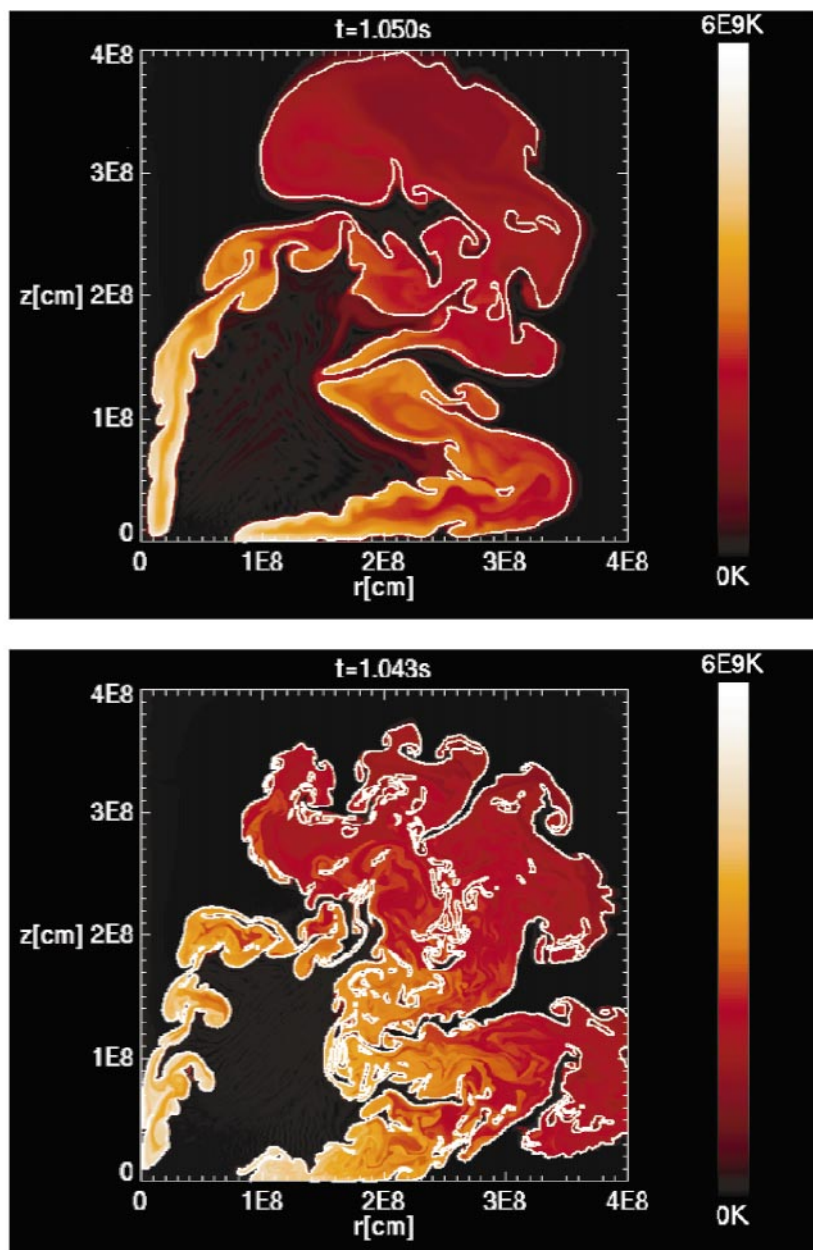


Figure 3 Snapshots of the temperature and the front geometry in a Chandrasekhar-mass deflagration model at 1.05 s (from Reinecke et al 1999c). Shown are a model with “low” resolution (256^2) (upper figure) and one with three times higher resolution, respectively. Because of the larger surface area of the better-resolution model, it exploded, whereas the other one remained marginally bound.



CONTENTS

A Fortunate Life in Astronomy, <i>Donald E. Osterbrock</i>	1
Stellar Structure and Evolution: Deductions from Hipparcos, <i>Yveline Lebreton</i>	35
The First 50 Years at Palomar, 1949--1999 Another View: Instruments, Spectroscopy, Spectrophotometry and the Infrared, <i>George Wallerstein and J. B. Oke</i>	79
Common Envelope Evolution of Massive Binary Stars, <i>Ronald E. Taam and Eric L. Sandquist</i>	113
The Evolution of Rotating Stars, <i>André Maeder and Georges Meynet</i>	143
Type Ia Supernovae Explosion Models, <i>Wolfgang Hillebrandt and Jens C. Niemeyer</i>	191
Extreme Ultraviolet Astronomy, <i>Stuart Bowyer, Jeremy J. Drake, and Stéphane Vennes</i>	231
X-ray Properties of Groups of Galaxies, <i>John S. Mulchaey</i>	289
Theory of Low-Mass Stars and Substellar Objects, <i>Gilles Chabrier and Isabelle Baraffe</i>	337
Organic Molecules in the Interstellar Medium, Comets, and Meteorites: A Voyage from Dark Clouds to the Early Earth, <i>Pascale Ehrenfreund and Steven B. Charnley</i>	427
Observations of Brown Dwarfs, <i>Gibor Basri</i>	485
Phenomenology of Broad Emission Lines in Active Galactic Nuclei, <i>J. W. Sulentic, P. Marziani, and D. Dultzin-Hacyan</i>	521
Mass Loss from Cool Stars: Impact on the Evolution of Stars and Stellar Populations, <i>Lee Anne Willson</i>	573
Winds from Hot Stars, <i>Rolf-Peter Kudritzki and Joachim Puls</i>	613
The Hubble Deep Fields, <i>Henry C. Ferguson, Mark Dickinson, and Robert Williams</i>	667
Millisecond Oscillations in X-Ray Binaries, <i>M. van der Klis</i>	717
Extragalactic Results from the Infrared Space Observatory, <i>Reinhard Genzel and Catherine J. Cesarsky</i>	761